Reevaluating the Runoff Mechanisms of Small Mountainous Catchments by Applying a New Storm-Runoff Model Based on the Vertical Unsaturated Flow

Makoto Tani[1)]

[1)]Former Graduate School of Agriculture, Kyoto University
Kitashirakawa Oiwake-cho, Sakyo-ku, Kyoto 606-8502 Japan
Corresponding Author E-mail : tanimakoto@nike.eonet.ne.jp

This paper is a translation from that in Japanese once published in Journal of Japan Society of Hydrology and Water Resources 36(1): 20-51, 2023. When citing, please follow the "Citation Notes" at the beginning of the paper n the next page.

Preface to Translation

In the runoff process on a hillslope, the rainwater movement changes from vertical to downslope direction due to the subsurface structure that becomes less permeable at deeper depths (See figure). Traditionally, physically-based runoff models have been developed assuming that the rapid temporal change in stream runoff rate (storm runoff response) during a large-magnitude storm event is produced by water movement in the downslope direction. However, I have long considered that vertical water movement may be the main controller of the response. The results of this consideration were summarized in a paper in Journal of Hydrology (Tani et al., 2020), co-authored with researchers in geomorphology and river hydrology.

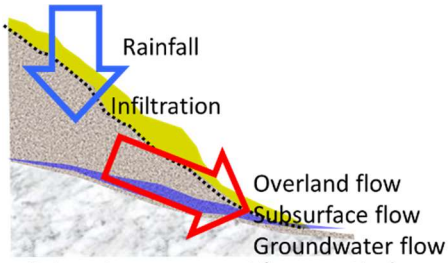

Rainwater movement from vertical to downslope direction

Based on the results of this paper, I developed a new runoff model for steep mountainous catchments in a tectonically-active region with a humid-temperate climate, and I published a paper on the model in Journal of Japan Society of Hydrology and Water Resources. I wanted to first convey the details of my intentions to Japanese researchers by expressing them in my native language, Japanese. Since I am not allowed to submit the same paper in its English translation to an international journal, and since I am already 73 years old, I decided to publish the translated paper on my personal homepage. Now that I have obtained the consent of the Society of Hydrology and Water Resources, the copyright holder, I am publishing it here.

This paper first incorporates a rather lengthy review of hydrologic runoff processes since John D. Hewlett in the 1960s to the present, and then discusses the significance of this paper in terms of the consistency that should be maintained between runoff mechanisms and runoff models. In the previous paper, Tani et al. (2020), I discussed the physical basis on which storm runoff response could be well simulated by runoff-storage relationship models, and the application results of runoff models to small catchments in this paper can take the discussion on the consistency between runoff mechanism and runoff model a step further.

As I stated at the end of the paper, I am convinced that this is a prerequisite for the development of runoff models physically-based on runoff mechanisms.

Reference

Tani M, Matsushi Y, Sayama T, Sidle RC, Kojima N. 2020. Characterization of vertical unsaturated flow reveals why storm runoff responses can be simulated by simple runoff-storage relationship models. Journal of Hydrology 588: 124982. DOI: 10.1016/j.jhydrol.2020.124982.

Appendix: Discussion with Keith Beven

Comments and discussions with Dr. Keith Beven on this paper are attached in https://hakulan.com/wp/wp-content/uploads/2024/02/Discussion-with-K.-Beven-2.pdf

I wish to express my deepest gratitude to him.

Reevaluating the Runoff Mechanisms of Small Mountainous Catchments by Applying a New Storm-Runoff Model Based on the Vertical Unsaturated Flow

Makoto Tani[1)]

[1)]Former Graduate School of Agriculture, Kyoto University
Kitashirakawa Oiwake-cho, Sakyo-ku, Kyoto 606-8502 Japan
Corresponding Author E-mail : tanimakoto@nike.eonet.ne.jp

Citation Notes

This paper was translated by the author, Makoto Tani, from a paper in Japanese with English abstract published in Journal of Japan Society of Hydrology and Water Resources, in the Vol. 36, No. 1 (2023), P.20-51 and posted on his personal website: https://hakulan.com/wp/. This translation was done using the results of translation by DeepL. The author thanks the society, the copyright holder, for the permission.

When citing, please use the following statement:

Tani, M. 2023. Reevaluating the runoff mechanisms of small mountainous catchments by applying a new storm-runoff model based on the vertical unsaturated flow. Journal of Japan Society of Hydrology and Water Resources 36(1), 20-51, 2023. (In Japanese with Englis abstract. Cited from English translation placed on Tani, M's personal web site: https://hakulan.com/wp/.)

ABSTRACT

A new runoff model was proposed based on the results of a study in which storm runoff responses were determined mainly from vertical unsaturated flow. Application of this model to three small mountainous catchments yielded good results for storm-runoff responses. These results suggest that soil-layer depth and soil physical properties play dominant roles in storm runoff responses. Runoff mechanisms were reevaluated based on model-application results and earlier observation studies. The variable source area concept was examined first: the runoff rate was quite low when the areas with wet condition in the entire soil layer were still horizontally isolated, but a high rate was achieved after the wet areas became mutually connected. A good simulation result obtained from the model application until landslide occurrence in a zero-order catchment suggests that presumably vertical water flow strongly affects storm runoff responses because the high groundwater drainage capacity is sufficient to maintain soil layer stability for several hundreds of years. Observed storm runoff rates from a weathered granite catchment with a large storage capacity in the bedrock were well simulated by about half of the rate calculated using the runoff model. This result suggests that the storm runoff response through the downslope flow might derive from the lower zone of catchment where the vertical unsaturated flow was intercepted by the shallow groundwater.

Key words: downslope flow, runoff contribution area, runoff mechanism, storm runoff model, vertical unsaturated flow

1. Introduction

In mountainous catchments, rainwater falling vertically on the ground surface is redirected downslope. The runoff process is divided into vertical flow, downslope flow, and channel flow. The author has emphasized that the vertical flow process plays an important role in storm runoff response (Tani, 1985a; Tani et al., 2020). In this paper, a conceptual runoff model is proposed based on this idea. Although this is a lengthy introduction, we review studies about storm runoff processes and explain the position of the model developed in this paper.

1. Vertical and downslope systems

On the earth, water vapor produced by seawater evaporation is transported over the land surface to fall precipitation, which is then discharged into rivers and returned to the sea. In this process, near the boundary between the atmosphere and the ground surface, downward precipitation occurs due to gravity and upward water vapor transport occurs due to atmospheric turbulent diffusion. The spatial scale of mountainous catchments is smaller than that of atmospheric phenomena, and the influence of the internal ground-surface topography on the spatio-

temporal distribution of precipitation is small (Tani, 1996). Therefore, the runoff process in a catchment begins with a nearly homogeneous horizontal vertical flux as a land surface boundary condition. The topography and subsurface structure of mountainous catchments are developed by weathering and erosion of the mountain bedrock formed by tectonic and volcanic activity. Therefore, the permeability of the ground structure generally decreases with depth. As a result, the flow of rainwater is constrained by these conditions structure and forced to divert from a vertical to a downslope direction. Downslope-directed stream channels form a dendritic network through erosion processes and repeatedly merge into a single stream channel that corresponds to the trunk of a tree (Tsukamoto and Ohta, 1988). Accordingly, as shown in the schematic diagram in Fig. 1, the runoff process in a mountainous catchment consists of a vertical system at the entrance and a downslope system concentrated at a single point at the exit, with a switch in the middle of the system.

Although this might go without saying, the author would like to emphasize the importance of this switch of direction in hydrology and try to explain why it is important. Vertical system has been emphasized in studies of evapotranspiration and baseflow, but for storm-runoff generation, they have been often regarded rather as "losses" that do not contribute to runoff (Takasao and Shiiba, 1988; Shiiba et al., 2013). The reason for the neglect of the vertical system may be due to its smaller spatial scale compared to the downslope system, but the author believes that storm-runoff response is mainly dominated by the vertical system. To understand this point, it is necessary to go back to the pioneer studies of hillslope hydrology in the 1960s. Note that “storm flow” in this paper refers to runoff that increases or decreases rapidly in response to rainfall, as distinguished from “baseflow”.

Hewlett and Hibbert (1967), citing soil column experiments with tritium (Horton and Hawkins, 1965), explained the concept of variable contribution area in storm runoff mechanisms by considering that

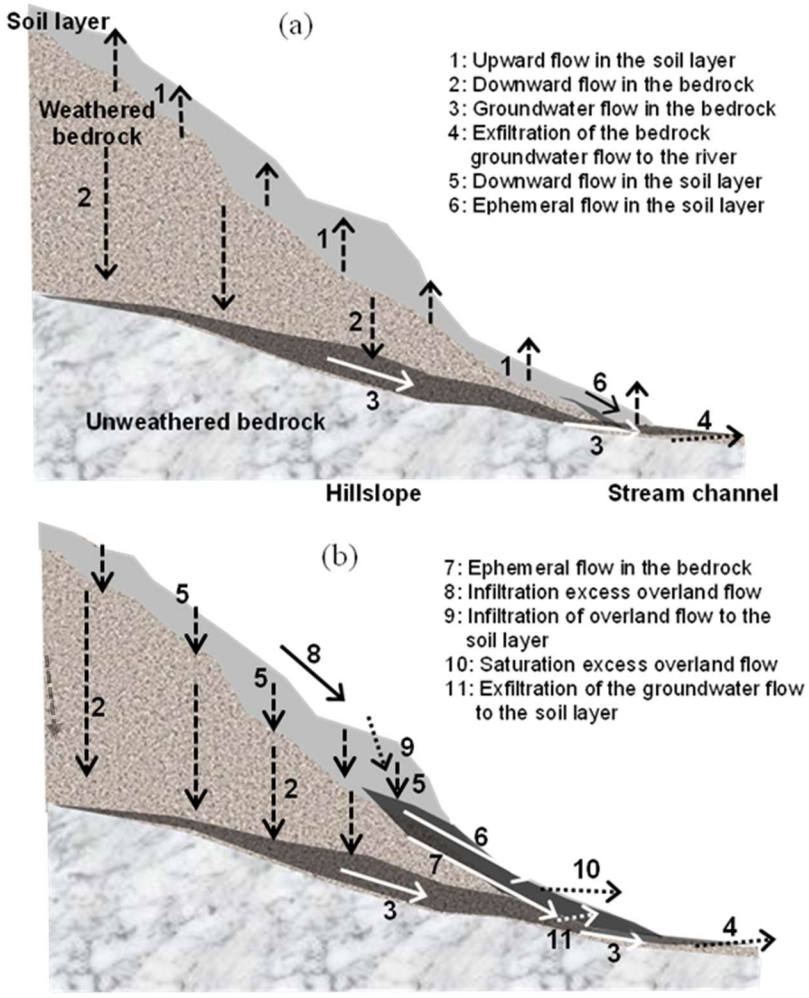

Fig. 1. Schematic showing runoff mechanisms for a mountainous catchment.

(a) Non-rain period. (b) Period when the soil layer is sufficiently wet because of the large amount of cumulative rainfall. Broken, solid, and dotted arrows respectively indicate vertical-flow system components, those in the downslope-flow system, and interchange flows between upper and lower layers.

new rain water pushes ahead old water included in the soil layer before the storm. Freeze (1972), on the other hand, conducted pioneering three-dimensional numerical experiments applying the Richards equation to the soil matrix to study runoff processes on hillslopes, and found that the slow flow in the slow-velocity downslope flow derived from general values of saturated hydraulic conductivity could not explain storm runoff responses, arguing that they were produced by saturation-excess overland flow generated by rising groundwater levels in the soil layer.

However, the soil layer on natural slopes is not composed solely of a soil matrix as assumed by Freeze (1972) but is very heterogeneous, containing a series of large pore spaces and pipe-like preferential pathways. Subsequent tracer studies have shown that river water during storm runoff does not consist of "new water" (i.e., rainwater flowing directly into the river), but rather a high proportion of "old water" that had been stored in the soil prior to the rainfall event (Sklash and Farvolden, 1979). Therefore, the fact that "old water" is the main source of storm runoff, and what kind of runoff mechanism it is based on, has been continuously discussed in the international hydrologic community (McDonnell, 1990; Anderson et al., 1997; Gomi et al., 2010). However, the question posed by Hewlett and Hibbert (1967) and Freeze (1972), namely, "Where is the rapid storm runoff response to rainfall produced?" has yet to be precisely resolved (Tani, 2013).

Among the many studies on this issue, those that are closely related to this paper are: #1 studies showing that the propagation of pressure head in a vertical system is rapid enough to generate storm runoff in wet soils, and #2 studies showing the importance of high velocity in preferential pathways in a downslope system. The following is a brief explanation of the two studies.

Regarding #1, Tani (1982; 1985a; 1985b) performed numerical calculations using the one-dimensional vertical form of the Richards equation, considered applicable to soil matrices, and showed that moist soils rapidly transmitted temporal variations in rainfall to the deeper parts of the soil. Ohta et al. (1983) demonstrated this theoretical result in an artificial rainfall experiment on a very small slope. It has been elucidated that rapid propagation of pressure head occurs even in soil matrices without preferential pathways, and that the temporal variation of rainfall is transmitted to the deep soil layers at a rate commensurate with the storm runoff response.

The characteristics has been demonstrated in a sprinkling experiment conducted in a steep-gradient zero-order catchment (CB1) at the Mettman Ridge study site (MR) in Oregon, USA. That is, vertical infiltration within the soil pushed water molecules out (Torres et al., 1998), and the temporal variation of rainfall was found to be rapid, even though the velocities measured by tracers were very small (Anderson et al., 1997). This result implies that there is a large difference between velocity and celerity in the soil-water movement, and its hydrological importance has recently been discussed (McDonnell and Beven, 2014).

Regarding #2, studies have focused on pipe-like preferential pathways in the soil (Mosley, 1982; Kitahara, 1992; 1993; Sidle et al., 1995; Uchida et al., 2003). Among them, information from tracer experiments conducted by Anderson et al. (1997) during a sprinkling experiment at CB1 was particularly important, revealing a fractured rock near the surface of the weathered bedrock below the soil layer, with rapid drainage through the pathways consisting of connected fractures.

When we have accepted the findings of both #1 and #2, the combination of high-celerity extrusion of water molecules in a vertical system and high velocity flow in a downslope system can sufficiently explain the storm runoff response, even if overland flow does not necessarily occur. According to this mechanism, it is not surprising that river water contains a large amount of "old water" unless all the soil water is pushed out by rainwater.

By distinguishing between vertical and downslope systems and considering the runoff mechanism as a combination of the two, it is possible to hydrologically examine the problem of Hewlett and Hibbert's (1967) idea, namely, that the temporal variation of the flow at the top of the slope is quickly transmitted to the bottom by the extrusion of water in the soil layer. Since this is important for discussing runoff mechanisms in heterogeneous soil layers, the main points are discussed here.

Note that rainfall events can range from light to heavy, and their intensity, except for drizzle, is in the range of 1 to 100 mm $h^{-1,}$ which is much smaller than the range of soil hydraulic conductivities for the unsaturated zone. Since the hydraulic conductivity of dry soil is much lower than the intensity of light rainfall, rainwater cannot flow smoothly to the deeper parts of the soil after rainfall begins, and a large increase in volumetric water content occurs near the ground surface, forming a wetting front. The downward progression of the front causes all rainwater to be stored in the soil pores until the wetted area extends deeper into the soil layer, which is a loss to storm runoff. However, when the soil layer becomes wet and the hydraulic conductivity increases to the range of rainfall intensities mentioned above, the effect of the gravity term in the Richards equation no longer requires a large increase in water content to allow rainwater to infiltrate deep into the soil (Tani, 1982; 1985). In this paper, ‘complete wet condition’ (hereafter referred to as CWC) is defined as the complete wetting of the soil

layer, where the hydraulic conductivity is within the range of rainfall intensity from the surface to the bottom. However, because the moisture content fluctuation is small, the temporal variation of rainfall is quickly transmitted to the deeper soil layers by pushing out the soil water, resulting in a significantly larger celerity than velocity.

It is important to note, however, that unlike a closed conduit flow, vertical unsaturated flow does not simply push water downstream. In contrast, in the unsaturated zone, changes in hydraulic conductivity are accompanied with those in volumetric water content, so that temporal variations in rainfall are not directly transmitted to the deeper soil layer, but are gradually equalized through changes in storage volume. As a result, the equalizing effect of temporal variations is produced through storage fluctuations in the soil layer, but the propagation speed becomes rapid unlike the case where a dry area remains within the soil layer. The fact that this phenomenon can be consistently explained by Darcy's law is an important theoretical characteristic of the vertical unsaturated flow (Tani, 2018).

On the other hand, since the flow in the soil matrix in a downslope system is primarily unconfined groundwater, an increase in the drainage intensity from the vertical system cannot increase the water content because the pore space is saturated. Therefore, fluctuations in the flow rate will always cause a rise or fall in the groundwater table, just as in an open channel (Tani, 2008). Therefore, when the drainage rate from a vertical system is high, the water surface rises toward the bottom of the slope, and with an increase in cumulative rainfall, saturated overland flow is likely to occur, as Freeze (1972) has shown in his numerical experiments. In the first place, the experiments of Horton and Hawkins (1965) were conducted on a vertical system, which is the reason for the rapid transmission of temporal changes in rainfall by soil water extrusion. Since unconfined groundwater flow in a downslope system does not cause soil water extrusion without a rise in the water surface, the explanation for the rapid storm runoff response within the soil layer in the downslope system as claimed by Hewlett and Hibbert (1967) must be rejected.

When preferential pathways exist in the soil layer and flow within them function as closed conduit flow, however, the rise of the groundwater flow can be suppressed by the increase of flow rate, as explained by Tsutsumi et al. (2005a; b) in their hydraulic analysis of experimental results on pipe flow in the soil layer. Groundwater levels may rise due to the limitations of the drainage capacity of the preferential pathways if rainfall magnitude is very high. Nevertheless, the drainage effect of preferential pathways must be emphasized at least in considering the storm runoff response of a downslope system.

Thus, in the subsurface structure of mountainous catchments, the combination of rapid propagation of rainfall fluctuations to the depth by the soil matrix in the vertical system and rapid drainage through preferential pathways in the downslope system will play a major role in the storm-runoff generation process. This mechanism is fundamental both to understanding runoff mechanisms in spatially heterogeneous hydrological media and to developing physically-based runoff models that must concisely represent them.

2. Understanding storm runoff response based on the theory of vertical flow

Tani et al. (2020), based on the results of the above study on runoff mechanisms, conducted numerical experiments to elucidate the physical basis for why storm runoff responses can be simulated by simple storage relationship models. In this paper, we propose a runoff model based on the vertical system and apply it to several small catchments, so we would like to introduce two themes from the results obtained in Tani et al. (2020).

The first theme points out the importance of a fixed proportion of rainfall allocated to storm runoff in a CWC. In the past, Hewlett and Hibbert (1967) proposed “variable contribution area concept,” which stated that storm runoff occurred in a portion of a catchment when rainfall began and that the contributing area expanded with an increase of cumulative rainfall, This has become a basic concept in hillslope hydrology through the accumulation of observational studies (McDonnell, 2009).When this concept was first discussed, it was common knowledge in runoff analysis that the contribution area extended over the entire catchment when flood-causing rainfall events were targeted in Japan, where steep topography and large rainfall events frequently caused severe floods and sediment hazards. The storage function model developed in 1961 proposed the concept of saturation rainfall, and it was recognized that when cumulative rainfall exceeded this value, the total volumes of new rainfall and storm runoff were almost the same, expressed in runoff rate per unit catchment area (Kimura, 1961; 1978; Padiyedath et al., 2018). The important point to understand from this is the finding that "as accumulated rainfall increases, the area contributing to runoff is fixed to the area of the entire catchment," and Tani et al. (2020) defined the CAP (constant allocation period) as the period during which almost all rainfall is allocated to storm runoff.

Indeed, Supraba and Yamada (2015) analyzed data from 36 mountainous catchments in Japan and found 23 catchments where most of the rainfall was allocated to storm runoff. However, this was not the case for the remaining 13 catchments within the range of cumulative rainfall observations.

For example, there are catchments where vertical infiltration into the bedrock continues. Even if this must be taken into account, the estimation of effective rainfall and the prediction of storm runoff are much easier during the period when the contribution area does not change. Therefore, the concept of a CAP is important as a clue for analyzing complex runoff mechanisms.

The above property, in which the total rainfall and the total storm runoff are almost equal in the CAP, has been often believed as "the soil layer becomes saturated and the storm mitigation function by the soil layer reaches its limit," influenced by the term "saturated rainfall" in the storage function model (Science Council of Japan, 2001; Laurance, 2007; Takahashi, 2019). However, this is not reasonable in terms of the runoff mechanism. As explained in the previous section, this CAP is established when the soil layer remains unsaturated but fully moist throughout the catchment, and does not mean that the soil layer is saturated. Therefore, the storm runoff mitigation effect of forest soils found by Kosugi (1999) in vertical unsaturated flow, where the decrease of peak-runoff rate is greater for crumb-structure forest soils, is maintained even when cumulative rainfall exceeds saturated rainfall (Science Council of Japan, 2011; Tani et al., 2020).

The second theme in Tani et al. (2020) was to show the physical reason why the conversion process of temporal variation in rainfall intensity to that in runoff rate in a CAP can be approximated by the basic equation of the storage function model. For a CAP, the effective rainfall is equal to the observed rainfall. Therefore, the problem to be considered in storm runoff response can be attributed to the conversion process from temporal variation of rainfall intensity to that of runoff rate (hereafter referred to as runoff conversion process) in case that the runoff volume is equal to the rainfall volume. The fact that this process can be simulated by the following basic equation of the storage function model has been widely recognized as a highly generalized knowledge based on many application results using this model (Sugiyama and Kadoya, 1988; Sugiyama at al., 1997; Supraba and Yamada, 2015).

$$S = kq^p \quad (1)$$

$$\frac{dS}{dt} = r - q \quad (2)$$

where r is the rainfall intensity, q is the runoff rate, S is the catchment storage, and k and p are empirical parameters.

The expression of runoff conversion process using this relationship between storage and runoff is employed not only for the storage function model but also for many runoff models with acceptable simulation results, such as the tank model (Sugawara, 1985), TOPMODEL (Beven and Kirkby, 1979), and HYCYMODEL (Fukushima, 1988; Fukushima and Suzuki, 1985; Tani et al., 2012). The main objective of Tani et al. (2020) was to explain the physical basis of this equation based on the Richards equation governing flow in vertical systems.

In Tani et al. (2020), as the first analysis of this second theme "runoff conversion process in CAP", rainfall, runoff, and pressure head observations (TY1 described below) on the valley-side slope (SL) of the Tatsunokuchi-yama Experimental Forest (TY), which is also addressed in this paper, were compared with the numerical results of applying the Richards equation to a vertical soil column. The results showed that the calculated pressure head values in CAP well simulated those observed, and the calculated drainage rate from the bottom of the soil column represented the observed runoff rate discharged from slope. These results support the hypothesis that the runoff conversion process in CAP is produced mainly from the vertical system, rather than from the downslope system.

The second analysis of the theme on runoff conversion process was conducted from the viewpoint of why the runoff rate and the total storage in the soil layer can be related by Eq. (1). The reason for this question was obtained from a result that the vertical system mainly occurred in the unsaturated zone and the effect of large-size pores on the water movement there was much smaller compared the effect in the saturated zone. Based on this interpretation, it was argued that the physical basis of equation (1) was likely to be the vertical system rather than the downslope system. Since this is an important point that demonstrates the role of the vertical system, let us explain it further.

In the case of downslope flow of unconfined groundwater, if we can assume a homogeneous soil layer without preferential pathways, it would be possible to obtain an approximate functional relationship between runoff rate and groundwater storage in the saturated zone, as discussed by Fujita (1981) and Harman and Sivapalan (2009). However, in saturated zones with positive water pressure, water flow tends to concentrate in pipe-like preferential pathways that have less resistance to flow than the surrounding soil matrix (Tsutsumi et al., 2005a; b). Therefore, even small changes in the storage volume in and around a preferential pathway will have a large effect on the runoff rate, while large changes in storage volume in an area without the pathway will cause little change in the runoff rate. When the preferential pathway functions as a closed conduit, as described earlier, the cross-sectional area of the flow does not change, so the storage volume does not change, and the runoff intensity is determined only by the flow velocity in it. Therefore, in soil layers containing preferential pathways, the relationship of the total runoff rate to the total storage obtained by simply integrating the water volume included in the saturated soil-matrix zone, unsaturated soil-matrix zone, and preferential pathways

over the entire soil layer, must be extremely complicated and may be unlikely to have a smooth functional relationship as in Equation (1).

On the other hand, in the unsaturated state, large pores have low capillary forces, and thus preferential pathways are filled with water only when they become saturated. Therefore, pathways cannot play main role in the unsaturated flow. Even in the unsaturated state, there is certainly film flows along the wall of preferential pathway (Beven and Germann, 2013), but it is unreasonable to consider this as the main pathway in a CWC. Therefore, in the unsaturated zone, water fills the small pores with high capillary force on a priority basis ubiquitously included in a soil layer even with preferential pathways. As a result, vertical flow in the unsaturated zone can be described by Darcy's law for the soil matrix.

Therefore, when the flow rate in the soil surface due to rainfall or other factors, the resulting changes in local volumetric water content propagate to the entire soil layer due to the effect of the diffusion term in the Richards equation, and this propagation causes changes in the water storage volume in the soil layer (Tani, 1982). In fact, Tani et al. (2020) obtained a relationship between storage volume and runoff rate similar to that of equation (1) from numerical experiments in the unsaturated zone of a vertical system, whether the soil layer is homogeneous or contains multiple physical properties. As described above, the difference in hydraulic properties between saturated and unsaturated zones has a decisive influence on whether the storage volume of the entire soil layer dominates the runoff rate.

The third analysis of the runoff conversion process examined what physical properties are reflected by the exponent p in equation (1). Many previous studies have assumed that the Manning equation describing overland flow can control the value of p, based on the result that its value is distributed around 0.6 derived from the optimization process in runoff analysis and that the physical basis for this can be found in the downslope system (Sugiyama and Kadoya, 1988; Fujimura et al., 2016). However, as shown by observations of hillslope hydrology, it is unrealistic to consider overland flow as the primary mechanism for producing storm runoff (McDonnell, 1990; Montgomery et al., 2009; Iwasaki et al., 2015). Some studies have also raised a question for the traditional view that unconfined subsurface flow in a sloping soil layer is linear and p=1, and have attempted to find reasons for the nonlinearity expressed as p<1 (Takagi and Matsubayashi, 1979; Harman and Sivapalan, 2009), but have not yet been able to explain runoff conversion process in the storm runoff responses.

In contrast to these studies, which seek the basis of the exponent p in the flow of a downslope system, Tani et al. (2020) argue that the value of p can be determined in a *vertical* system rather than in a *downslope* system. First, they define the dimensionless quantity δ as the ratio of the depth of the vertical soil column to the absolute value of the physical quantity ψ_m (included in equation (5) below, which is the value of the pressure head corresponding to the median value of the log-normal distribution function of the soil pores). It is elucidated that p becomes smaller with a larger δ and approaches 1 with a smaller δ. For example, for the same soil layer thickness, a loamy soil rich in small pores has a smaller δ value, which corresponds to near 1 value for p because of the larger absolute value of ψ_m compared to a forest soil or a sandy soil that contains many large pores. For the same soil physical properties, it is suggested that when the soil layer is thick, δ becomes large and p becomes small with a high nonlinearity.

3. Significance of developing a runoff model based on vertical flow

As explained above, Tani et al. (2020) proposed that "as the cumulative rainfall increases, CWC area spreads and finally reaches CAP. During this period, the runoff conversion process can be expressed by equation (1) of the storage function model, but its physical basis is the vertical flow system to which the Richards equation can be applied". Therefore, the author has decided to develop a runoff model based on the role of the unsaturated flow in the vertical system (vadose zone runoff model, hereinafter abbreviated as VZ model). The advantage of this model is that *it can predict the effects of soil physical properties and soil layer thickness on the runoff conversion process in the storm runoff response.*

More importantly, it has the potential *to bridge the large gap that exists between observational and modeling studies in hydrology*. In general, observation and modeling should be the means to understand natural phenomena, but there has been a tendency for two separate research groups to work in parallel in the case of runoff phenomena (i.e., scientific research to understand the mechanisms through observation and engineering research to predict the response of runoff to rainfall with greater accuracy by developing new runoff models). The author understands that solving this problem was one of the important goals of the Japan Society of Hydrology and Water Resources when it was founded in 1988, but it still remains a challenge because the significant heterogeneity included in runoff phenomena causes difficulty for the development of physically-based runoff models (Sivapalan, 2003; Tani, 2013; 2016). Therefore, in this paper, the author not only applies the VZ model to the observed data of small catchments, but also tries to reevaluate the runoff mechanism by comparing the results of the application with the

previous observational results in the same catchments.

An additional issue has been also presented how to distinguish the effects of the slope system and stream-channel system on the storm runoff responses in mountainous catchments. For the latter effect, the latest study by Asano et al. (2020), which observed the occurrence time of storm-runoff peaks at many points along a stream channel, provided important information: delay in the occurrence time is caused by the stream-channel system, and almost no delay was created from the slope system. This means that the runoff conversion process is produced mainly by the vertical flow in the slope system, and the peak delay is produced mainly by the stream channel. As a result, it means that the downslope flow system between the two kinds of flow systems has little effect on either the runoff conversion process or the peak delay included in rainfall-runoff responses. Although further analyses of a large number of observation data is necessary, the author believes that the VZ model based on the vertical flow system, which ignores the effects of the downslope and channel flow systems on the storm runoff responses, is of great significance for hydrological phenomena in small mountainous catchments.

II. Overview of runoff model

1. Model development design

Figure 1 shows the main components of the runoff mechanism for vertical and downslope systems in mountainous catchments. This figure depicts downslope flow components in the layered structure, such as surface flow and subsurface flow, but also the components of exchange flow between the upper and lower strata are depicted with awareness. The actual runoff mechanism is much more complex and contrasts sharply with the simplicity of the runoff model. This section describes how this complex runoff mechanism can be reflected in a VZ model based on a vertical system.

In mountainous catchments under humid temperate climate such as Japan, the subsurface structure on a hillslope is composed of a forest soil layer at the surface, which transitions through weathered to unweathered bedrock, unless it is severely disturbed by volcanic activity or human activity. The soil layer, called the vadose zone, is repeatedly dry and wet, reflecting climatic conditions (Hopmans and van Genuchten, 2005). On the other hand, weathered bedrock is less susceptible to evapotranspiration and maintain near saturated condition.

The VZ model simplifies this complex subsurface structure and water movement and assumes that preferential pathways are distributed near the boundary between the soil layer and weathered bedrock

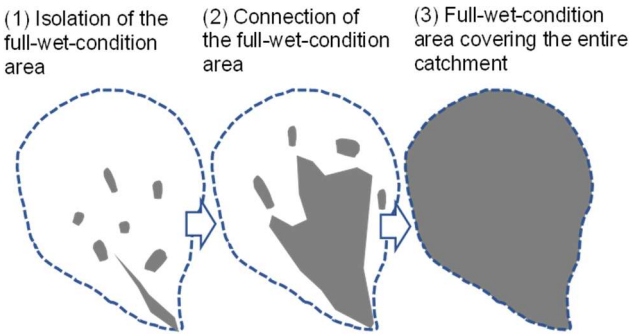

Fig. 2. Schematic showing expansion of the source area from the viewpoint of the connection of full-wet-condition area in response to increased cumulative rainfall.

and that groundwater drains quickly through them. The model also assumes that the water table does not rise and the thickness of the unsaturated zone remains constant, even after the soil layer has reached CWC due to enough rainfall supply. In reality, it must be considered that even if drainage is efficient, a large rainfall will cause the water table to rise, pushing the unsaturated zone toward the ground surface and decreasing the thickness of the vertical system. Therefore, fixing the thickness of the unsaturated zone is only an assumption in the model.

In addition, the VZ model assumes that the physical properties of the soil layer are homogeneous within the watershed. Then, as the cumulative rainfall increases, the soil layer in the watershed becomes wetter from the plot with a small thickness. This plot early becomes contribution area to storm runoff, since a rapid runoff conversion process through the vertical system to the downslope system firstly occurs at this plot. However, as shown in Fig. 2 (1), which is a conceptual diagram of the expansion of the contribution area, when the CWC area is isolated, most of the flow in the downslope system is not connected to the stream channel, and the contribution area is limited to a small area around the stream. As the cumulative rainfall increases, the CWC area gradually becomes connected each other, as shown in Fig. 2 (2), and the contribution area expands toward the entire catchment. Observations that the expansion process occurs rapidly have already been obtained, and the concepts of threshold and connectivity have been noted in our hydrological community (Tani, 1997; Tromp-van Meerveld and McDonnell, 2006; Lehman et al., 2007; Anderson et al., 2009).

Tani et al. (2020) only dealt with runoff conversion process during the CAP, as shown in Fig. 2(3), but the mechanism, by which the runoff conversion process is produced by the vertical system in limited areas that have become completely wet, is common even in the earlier stages. However, since the VZ model does not represent the flow of downslope

system, it is not possible to follow the process of the expansion of the wetted areas from scattered isolated areas to a larger area of runoff contribution. Therefore, in this paper, the VZ model is also applied to the process leading up to a CAP, and the calculated runoff rate is compared with the observed runoff rate in order to extract information on the process of expanding the contribution area.

The VZ model deals exclusively with vertical systems, but some of the vertical flow may pass through preferential pathways such as living or decaying roots, or paths of soil animals like earthworms. Therefore, even if there are still dry areas in the soil matrix, the flow through the preferential pathways often reaches the deeper soil layers and becomes wetter before the surrounding area (Noguchi et al., 1997; Liang et al., 2009; Beven and Germann, 2013). Some attempts have been made to develop a hillslope runoff model that emphasizes this point (Dusek et al., 2012). However, after the matrix portion of the soil layer receives enough cumulative rainfall to become completely wet, both the flow through the preferential pathways and the pressure propagation in the soil matrix play the same role in terms of rapid transmission of rainfall variation to the soil-layer bottom. Therefore, the VZ model ignores the influence of preferential pathways and considers only the vertical unsaturated flow processes in the soil matrix contained in all vertical cross sections.

In mountainous catchments, a distinction is usually made between slopes and channels. However, as in the zero-order catchment (CB1) of the Mettman Ridge study site cited earlier (Anderson et al., 1997) and the Kiryu Experimental Watershed (Iwasaki et al., 2015), which will be treated later in this paper, applying the distinction between the two on topographic maps to systems of flow in the sloping direction is not necessarily not appropriate. That is, observations in these catchments indicated that downslope flow within the subsurface structure including weathered bedrock exfiltrates to the soil layer and/or river channel to produce storm runoff responses (see Fig. 1). Therefore, as discussed in the previous section, this complex interchange of downslope flows should be considered as linking the CWC areas together. The VZ model calculations show that these areas are interconnected in the horizontal direction, and that the area contributing to the runoff is expanding. In the VZ model calculations, the complexity of the flow mechanism in the downslope system and its small contribution to the runoff conversion process system are taken into account, and it is assumed that the effect of flow in the sloping direction is neglected for the entire catchment, without distinguishing between slopes and channels.

2. Model algorithm

The algorithm of the VZ model is shown in Fig. 3. In step (1), a conceptual two-dimensional cross-sectional view is drawn, but in reality, the soil layers of the entire mountainous catchment including slopes and

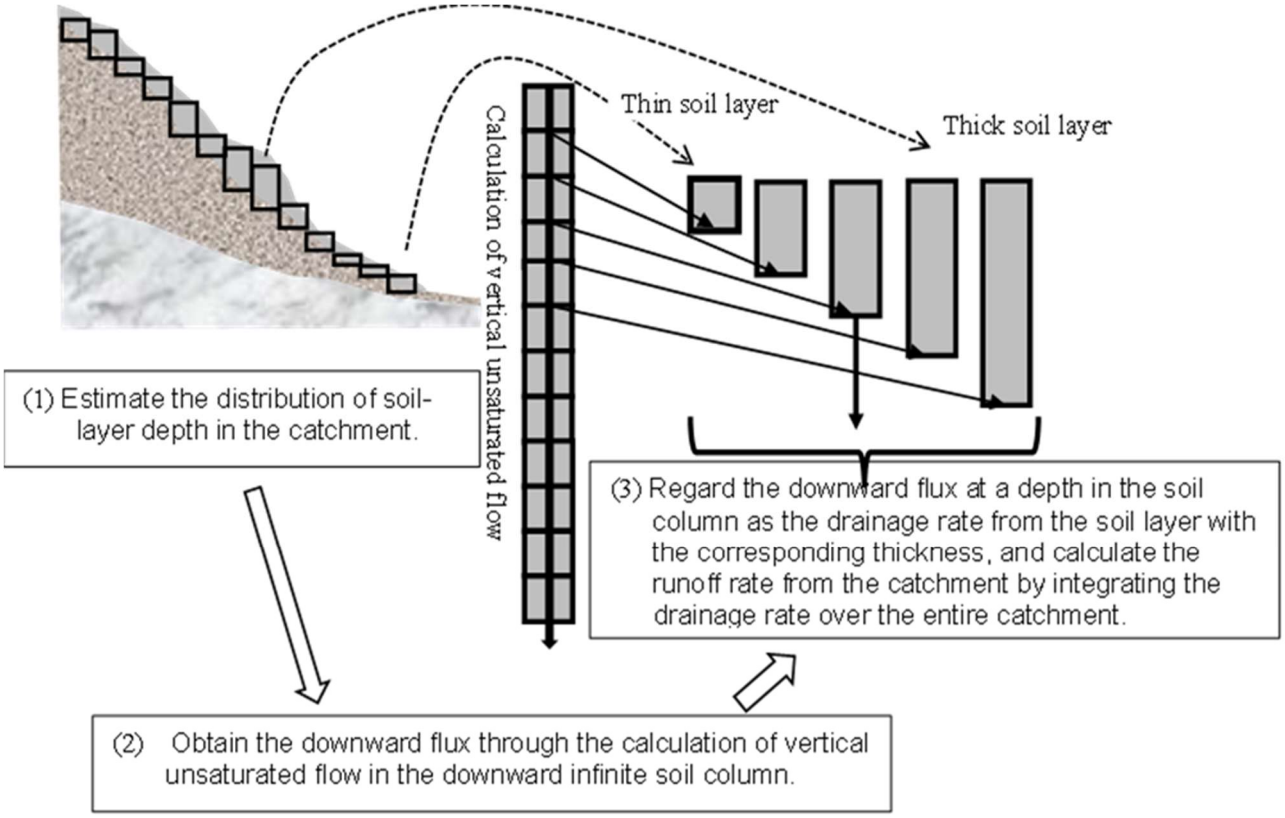

Fig. 3. Algorithm of the VZ model.

river channels are considered, and the drainage rate from the bottom of each soil layer is calculated. This is done by the vertical unsaturated flow calculation in step (2). Next, the runoff rate from the entire catchment is calculated in step (3), in which the drainage rate from the bottom of each soil layer can be simply integrated over the entire catchment since the effect of the flow in the downslope system is ignored. Therefore, the only catchment conditions involved in the runoff conversion process are the horizontal distribution of soil layer thickness and soil physical properties over the entire watershed.

The vertical system in step (2) of Fig. 3 is calculated assuming a semi-infinite length soil column with the top end at the ground surface. The Richards equation for vertical one-dimensional infiltration in a soil column can be written as follows.

$$C\frac{\partial\psi}{\partial t}=\frac{\partial}{\partial z}\left\{K\left(\frac{\partial\psi}{\partial z}-1\right)\right\} \quad (3)$$

where K is the hydraulic conductivity, C is the specific water capacity ($=d\theta/d\psi$), ψ is the pressure head, and t is time. The z-axis is positive downward with its origin at the ground surface. The boundary condition at the ground surface gives the rainfall intensity r.

$$f=r \quad (4)$$

where f is the vertical flux.

The inflow rate in a unit sectional area drained from each soil-layer bottom into a downslope flow is assumed to be equal to the downward flux f at a depth corresponding to the thickness of the soil layer in a semi-infinite length soil column. Assuming that the thickness distribution of the soil layer within the catchment is known, the runoff rate from the catchment can be calculated by integrating the drainage rate at each location over the entire catchment, as shown in step (3) of Fig. 3.

Now, the functional relationships for water retention and permeability, i.e., volumetric water content θ and hydraulic conductivity K with respect to ψ, which are required as soil physical properties, can be represented by the Kosugi equation (Kosugi, 1996), respectively, as follows.

$$\theta=(\theta_s-\theta_r)Q\left[\frac{\ln(\psi/\psi_m)}{\sigma}\right]+\theta_r \quad (5)$$

$$K=K_s\left[Q\left\{\frac{\ln\left(\frac{\psi}{\psi_m}\right)}{\sigma}\right\}\right]^{\frac{1}{2}}\times\left[Q\left\{\frac{\ln\left(\frac{\psi}{\psi_m}\right)}{\sigma}+\sigma\right\}\right]^2 \quad (6)$$

where θ_s and θ_r are the saturated and residual water contents, ψ_m and σ are the pressure head calculated from the median pore radius and is the standard deviation of the log-normal distribution of soil pore radius, respectively, and K_s is the saturated hydraulic conductivity, and Q is the complimentary normal distribution function.

Numerical calculations were performed using HYDRUS 1D (Šimůnek et al., 2013), which is widely used in soil physics. Since a semi-infinite length soil column is not practically feasible, the bottom boundary condition of a 10-m-long soil column was set to allow for deeper penetration (free drainage boundary condition in HYDRUS 1D), and it was confirmed that the effect of rainfall condition was not transmitted to the bottom during the calculation period. Depth increment was set at 2.5 cm. The spatial distribution of the thickness of the soil layer is not usually easy to obtain by field investigation, but the method of setting it up is described in the application to each catchment. Initial conditions are also described for each individual case.

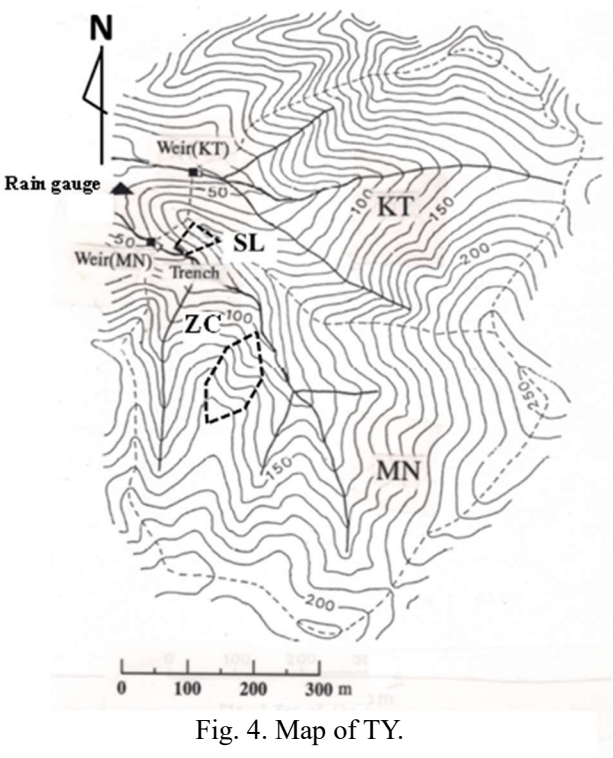

Fig. 4. Map of TY.

III. Site hydrological properties

Since three mountainous catchments are provided for our analyses in this paper, their basic properties are summarized. The characteristics of rainfall allocation to runoff in each catchment and an overview of the rainfall events to be analyzed is also described here.

1. Tatsunokuchi-yama Experimental Forest (TY)

The Tatsunokuchi-yama Experimental Forest (TY) consists of the 17.27 ha Kitatani catchment (KT) and the adjacent 22.61 ha Minamitani catchment (MN), and is located in a hilly mountainous area on the suburbs of Okayama City, Japan. It was established in 1937 to study the effects of drought on forests in the Seto Inland Sea climate with low rainfall, and hydrological observations are still being conducted by

the Kansai Research Center of Forestry and Forest Products Research Institute (Fig. 4) (Tani & Hosoda, 2012; Tamai, 2014; Tamai et al., 2020). The annual precipitation is 1,220 mm, and the mean annual temperature is 13.5°C. Most of both catchments are Paleozoic Formation, consisting of sedimentary rocks in sandy and muddy rock alternation, but over 30% of the KT and about 4% of the MN are quartz-porphyry rocks. Slope over these rocks tends to be steep, and the average slopes for KT and MN are 28.4 and 23.8, respectively. Soils in both geologies are clay loam, with thin soil layers on quartz-porphyry slopes and with thick on Paleozoic slopes (Tani, 1997; Hosoda and Tani, 2016).

In 1986, a 6 m long water collection trench was installed at the lower end of a steep quartz-porphyry valley-side slope (SL) along the stream channel in the MN catchment, and flow observation was conducted for about one year (Fig. 5) (Tani, 1997). The slope length is 42.7 m, the slope is 34.6°, the catchment area is 500 m^2, and the average thickness of the soil layer is about 50 cm.

Relation between the total rainfall and the total storm runoff for KT, MN, and SL in TY is shown in Fig. 6. The total storm runoff was calculated by simple hydrograph separation with a straight line connected from the point of initial runoff to the inflection point on the recession limb on a semi-logarithmic graph scale (Kadoya, 1979). This method was also applied to KI, described later. Since this method was used, the separated baseflow rate was added to the runoff rate calculated by the VZ model when comparing the calculated hydrograph with that observed.

In the case of events with the total rainfall generally smaller than 100 mm, the total storm runoff shows a noticeable variation due to the effects of dry and wet conditions in the catchment prior to the rainfall, but in events with larger cumulative rainfall, there is a tendency for the storm runoff to be allocated approximately equal to the newly fallen rainwater, i.e., a CAP, which is common to KT, MN, and SL (Fig. 6). However, the total storm runoff for large cumulative rainfall events tends to be slightly smaller in the order of SL, KT, and MN (Tani, 1997).

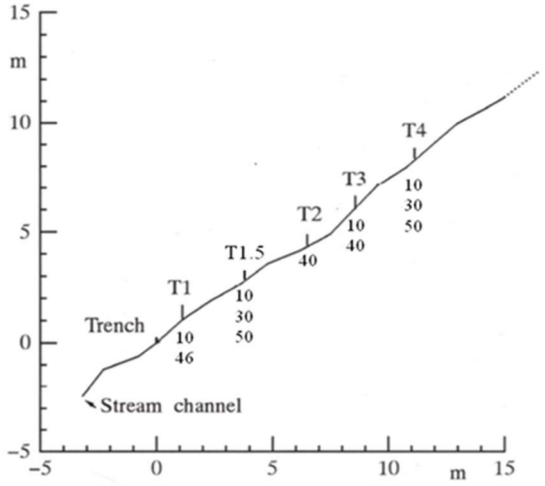

Fig. 5. Location of tensiometers in the profile of soil layer on the hillslope (SL) in MN.

Numbers represent depths in centimeters from the ground surface.

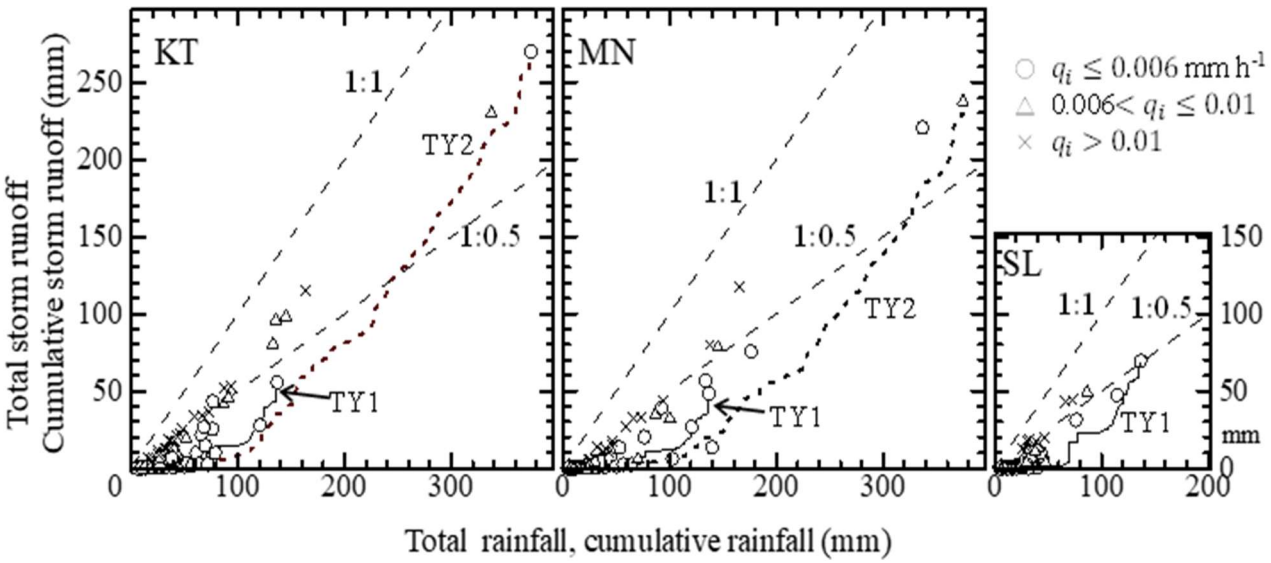

Fig. 6. Relation between the total rainfall and the total storm runoff for KT, MN, and SL in TY.
q_i is the initial runoff rate. Lines show the respective relations between cumulative rainfall and cumulative storm-runoff for storm events.

Modified based on work by Tani and Abe (1987) and Tani (1997).

Table 1. List of storm events

Event ID	Catchment	Storm event	Total rainfall	Duration	Maximum 24-hour rainfall	Maximum hourly rainfall[1)]	Total runoff	Maximum runoff rate
			mm	h	mm	mm h^{-1}	mm	mm h^{-1}
TY1	KT	Jul, 1987	131.5	131	52.0	14.5	54.7	2.30
	MN						47.7	1.40
	SL						69.2	4.00
TY2	KT	Sep, 1976	374.9	121	141.7	14.3	276.8	9.10
	MN						246.2	6.30
KIEX	Small slope (Plot 2)	1981	164.0	3	164.0	79.8	153.2	76.50
KI1	KI	Aug, 1982	348.9	58	295.0	30.0	173.7	14.90
KI2	KI	Jul, 2006	341.3	180	86.0	13.7	125.8	4.10
MREX	Upper weir for CB1	May, 1992	276.6	166	40.7	2.0	74.1	0.68
	Lower weir for CB1						76.1	0.69
MR1	Catchment including CB1[2)]	Nov, 1996	292.2	112	167.0	23.4	—[3)]	—[3)]

1) Maximum rainfall intensity in response to the maximum runoff rate
2) Total catchment including CB1 and its immediately west zero-order catchment
3) No data due to an occurrence of landslide

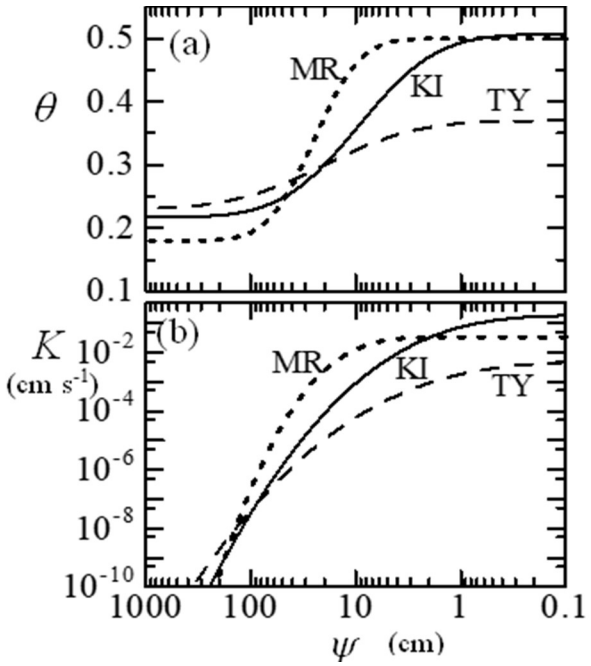

Fig. 7. Soil physical properties used for VZ model application.

Panel a shows the relation of θ (volumetric water content) to ψ (pressure head). Panel b shows the relation of K (hydraulic conductivity) to ψ.

Table 2. Parameter values of Kosugi's model for soils at each study site

Site	θ_r	θs	ψ cm	σ	K_s cm s^{-1}
TY[1)]	0.230	0.370	-20.0	1.60	5.0×10^{-3}
KI[2)]	0.212	0.507	-9.4	1.34	1.9×10^{-1}
MR[3)]	0.180	0.500	-25.0	0.80	3.4×10^{-2}

1) Tatsunokuchi-yama Experimental Watershed
2) Kiryu Experimental Watershed
3) Mettman Ridge Study Site including CB1 catchment

cumulative rainfall and cumulative storm runoff for the two rainfall events used in this paper. One is the July 1987 rainy season event (TY1), also used in Tani et al. (2020), for which SL, KT, and MN runoff rates and SL pressure hydraulic head are available. The other is the September 1976 typhoon event (TY2) for which KT and MN runoff rates are available. Both events lasted several days, but TY2 was considerably larger in magnitude than TY1, as shown in Table 1, which summarizes the rainfall events. The cumulative rainfall-runoff curve bends significantly at about 100 mm for KT and MN, and at about 70 mm for SL, indicating that almost all the amount of rainwater is allocated to storm runoff thereafter (Fig. 6).

The subsurface structure of SL is composed of weathered quartz-porphyry rock beneath a thin soil layer of about 50 cm, and storm runoff is estimated to be generated through pipe-like preferential pathways near the boundary between the soil layer and bedrock (Tani, 1997). In contrast, in the area of the Paleozoic Formation in KT and MN, the thickness of the soil layer that could be penetrated by a handy dynamic cone penetrometer was about 2.5 m from the middle to the lower part of the slope, and about 1 m from the middle to the upper part (Hosoda and Tani, 2016). In the Paleozoic Formation area where the soil layer is thick, it is difficult to estimate the runoff paths of the downslope system (see V.3).

Figure 7 and Table 2 summarize the water retention and permeability characteristics of the soils used in the VZ model calculations and named SB by Tani et al. (2020).

2. Kiryu Experimental Watershed (KI)

The deep weathered granite Tanakami Mountains, located south of Lake Biwa in Shiga Prefecture, used to be covered with devastated land formed due to intense human activities (Ohta et al., 2022). Hydrological observations by the Graduate School of Agriculture, Kyoto University, led by Yoshihiro Fukushima, began around 1970, mainly to evaluate the effects of revegetation work on hydrological processes. Especially in the Kiryu Experimental Watershed (5.99 ha, KI), which was restored to a mature cypress forest with good growth, studies were conducted mainly by Masakazu Suzuki, Nobuhito Ohte, and Yoshiko Kosugi, and various kinds of important results on forest hydrology have been obtained (Fig. 8) (Suzuki, 1980; Kubota and Sivapalan, 1995; Ohte et al., 1995; Kosugi et al., 2013; Sakabe et al., 2021; Katsuyama et al., 2021).The annual precipitation and the annual mean temperature in KI were 1,678 mm and was 13.4°C, respectively.

Masanori Katsuyama's group measured the spatial distribution of soil layer thickness by boring stick survey at 618 sites throughout the KI watershed (a handy dynamic cone penetrometer was used for sites larger than 2.5 m) (Katsuyama and Nagano, unpublished), compiled a frequency distribution with 0.25 m increments, and estimated the mean to be 0.65 m (Iwasaki et al. 2020). The reason for the thinness of the slope compared to natural slopes is assumed to be that the time elapsed after the revegetation work

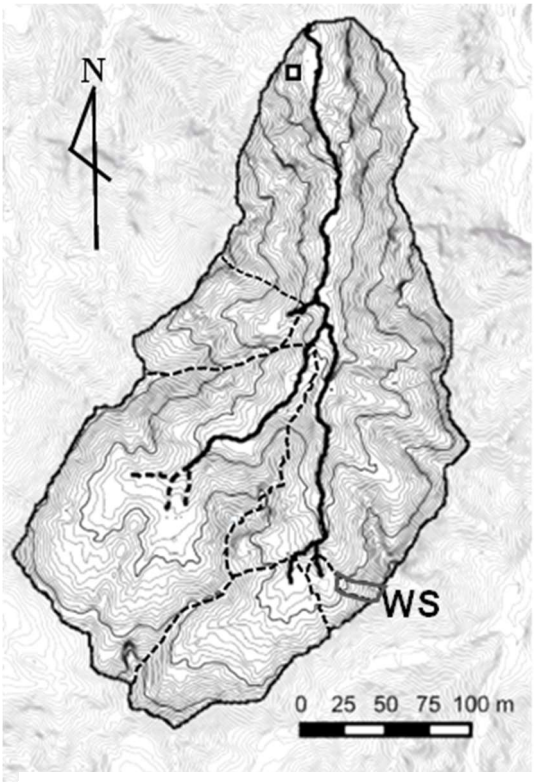

Fig. 8 Map of KI.

□: location (Plot 2) at which KIEX was conducted.

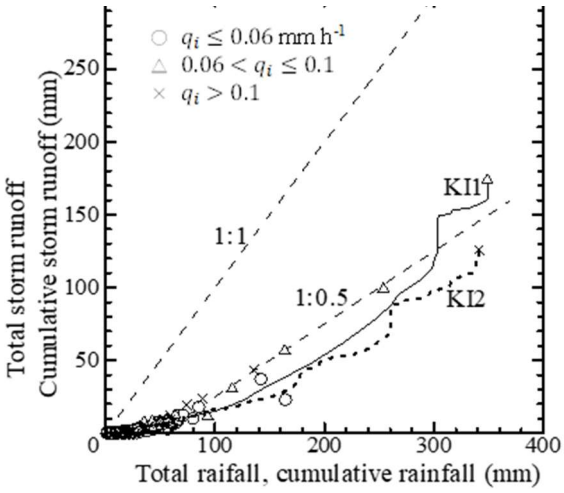

Fig. 9. Relations between the total rainfall and the total storm runoff for KI.

q_i and lines are the same as those in Fig. 6.
Modified based on work by Katsuyama *et al*. (2008).

conducted around 1917 was shorter than the period of natural development of the soil layer after the landslide in forested hillslope (Fukushima, 1987; Fukushima, 2006). Sediments eroded every year during the devastated-land period were thickly deposited upstream of the small check dam along the stream channel, contrasting with the thin soil layer on the steep hillslopes. Since the base rock is deeply-weathered granite, it has already been demonstrated through detailed water quality studies that a considerable amount of rainwater percolates deep into the bedrock and exfiltrates to the stream from the channel bed later (Katsuyama et al., 2005; 2010; Iwasaki et al., 2015).

Relation between the total rainfall and the total storm runoff for KI are shown in Fig. 9. Compared to the catchments in TY shown in Fig. 6, two characteristics can be pointed out: first, the total storm runoff variability is small due to the dryness of the catchment prior to rainfall, and second, a portion of the rainfall is not allocated to storm runoff even when the total rainfall is large, and a CAP is not observed. Fig. 9 also shows the relationship between cumulative rainfall and cumulative storm runoff for the two rainfall events. Both curves show a smooth shape meaning the rainfall allocation characteristics to the storm runoff and no clear bending point unlike shown in TY.

The VZ model was applied to a large-scale event (KI1) caused by Typhoon Bess in August 1982 (Tani et al., 1988), when a debris flow occurred in a steep torrent in the Tanakami Mountains, and a long rain event (KI2) during the rainy season in July 2006, when the spatiotemporal distribution of pressure head was observed in a zero-order catchment (WS) (Katsura et al., 2014) (Table-1). The slope length, mean gradient, and mean thickness of the soil layer in WS (240 m^2) are 28 m, 23.4˚, and 70 cm, respectively (Kosugi et al., 2006). Prior to them, the VZ model was applied to an artificial rainfall experiment (KIEX) for its verification which was conducted on a small slope Plot 2 (3 m wide, 3 m long, 32˚ slope) with a 50 cm thick soil layer on an impermeable bedrock in KI (Ohta et al., 1983).

The soil water retention and permeability properties required for the VZ model applications to the storm events including KIEX were obtained from soil surveys in WS (Katsura et al., 2014) (Fig. 7, Table 2). The soil is characterized by sandy soils with relatively large pores derived from weathered granite bedrocks.

3. Mettman Ridge study site (MR)

The Mettman Ridge study site (MR) in Oregon, USA, the bedrock of which consists of Eocene turbidite sandstone is situated in a tectonic zone with a humid climate similar to Japan, and the annual precipitation rate of approximately 1,500 mm (Torres et al., 1998). Detailed hydrogeomorphological studies were conducted at the site under the leadership of William E. Dietrich and David R. Montgomery (Fig. 10) (Montgomery et al., 1997). In particular, in CB1, a steep 860 m^2 zero-order catchment with an average slope of about 40˚, a sprinkling experiment with a low-intensity of about 1.65 mm h^{-1} continued for 7 days from May 27 to June 4, 1992, providing much hydrologic information, as quoted in I.1. More notably, the observation during a large natural rainfall event in November 1996 gave us valuable hydrologic data right up to the occurrence of the landslide within the CB1 catchment when the sensors were destroyed (Montgomery et al., 2009). In this paper, we attempt to apply the VZ model to the sprinkling experiment (MREX) and the observed result from the landslide-occurrence event (MR1).

In the entire 1.24 ha MR area, the thickness of the soil layer was investigated at 626 points and summarized in a frequency distribution in 0.25 m increments, ranging from a thin section of less than 0.25 m to about 2 m (Schmidt, 1999). The bedrock under the soil layer is composed of oxidized rock and fractured rock on the fresh rock (Anderson et al., 1997).

The lower end of the CB1 catchment was connected to channel head, and water bypassed through the fractured bedrock was exfiltrated from the channel bed. Two weirs were constructed for runoff measurement. The upper weir, located at the channel head, measured the runoff from the CB1 soil layer (Q_U), and the lower weir, located 15 m downstream, measured the runoff in the stream channel (Q_L). Although runoff from the zero-order catchment at the west of CB1 also joined the channel between the two weirs (Fig. 10), the design was such that runoff from the soil layers in both zero-order catchments did not

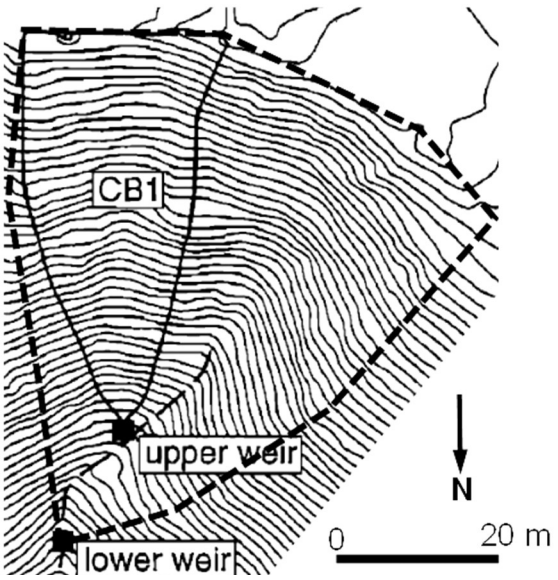

Fig. 10. Map of MR.

Modified based on work by Montgomery *et al.* (1997).

pass through the downstream weir. Therefore, it should be noted that in the case of natural rainfall MR1, only the flow that entered the channel between the two weirs was recorded at the lower weir, and that the total flow at both weirs did not include the runoff from the soil layer of the west zero-order catchment. Since MREX is a sprinkling experiment on the CB1 catchment only, the total flow represented the response to rainfall within the CB1.

Figure 11 shows the results of MREX to provide an overview of the observations. Fig. 11(a) plotting rainfall and runoff indicates that the flow rates at both weirs increase for three days after the start of experiment as the dry soil gradually becomes wetter but then reach nearly steady states. Thereafter, due to the evaporation of water supplied by the sprinklers and wind blowing, the intensity of the rainfall shows diurnal variations, which are larger during the night and smaller during the day, and this variation is clearly reflected in the flow rates at both weirs. The observed hydraulic head values (pressure head + potential head) at nest 5-4, slightly lower than the middle of CB1, during the MREX period are shown in Fig. 11(c), based on Ebel et al (2007). It can be seen that the diurnal variations are also reflected in the vertical propagation of the pressure head. Regarding the water balance during the steady-state water, Anderson et al. (1997) reported that, the 20% portion of the diurnal variation in rainfall intensity with an average value of 1.65 mm h^{-1} was lost by evapotranspiration and the rate of 0.3 mm h^{-1} infiltrated into the groundwater zone in the bedrock, and that roughly half of the remaining 1.0 mm h^{-1} or so was respectively measured at each of the upper and lower weirs (Figs. 11(a) and 11(b)).

During this steady-state period, water tracing experiments were also conducted for both vertical- and downslope-flow systems (Anderson et al., 1997). In the former, water labeled with deuterium was given as sprinkler water for two days only, and water samples were taken with a number of lysimeters of different thicknesses to determine velocities. The results showed that there was no bypass flow through the preferential pathways, and that the flow velocity was small, about 5-7 mm per hour, pushing out the soil water on the deeper zone. On the other hand, the velocity of the downslope flow through the bedrock fractures was also measured by injecting bromine ions into the saturated zone, and a large velocity of about 7-15 m per hour was obtained. The above results revealed that this steady period could be regarded as an approximate CAP although deep infiltration continued to occur, and that the diurnal variation of the input rainfall was quickly transmitted to the stream runoff by the extrusion of soil water in the vertical system and the quick flow through the fractures in the downslope system.

The soil physical properties in Kosugi equation required for the VZ model applications,

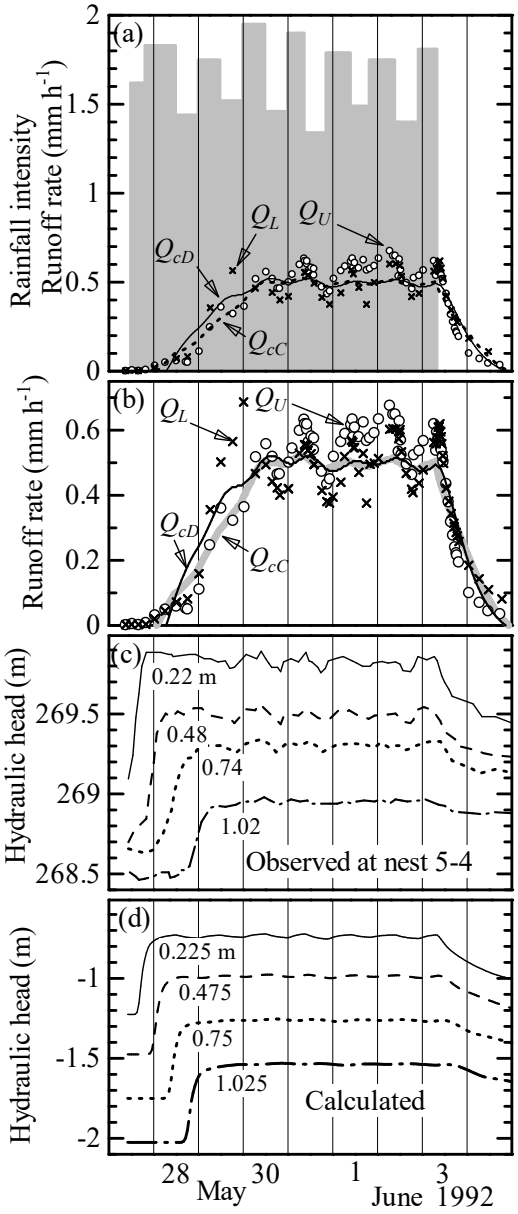

Fig. 11 Comparison of runoff rate calculated using the VZ model and that observed for a sprinkler experiment (MREX) in CB1 of MR.

Panel a shows the observed rainfall intensity and the observed and calculated runoff rates. Q_U and Q_L respectively represent the observed runoff rates from the upper and lower weirs, whereas Q_{cD} and Q_{cC} respectively denote the runoff rates calculated using the investigated and linear distributions of soil-layer depth. Panel b was shown to clarify the comparison of runoff rates. A different symbol was used for Q_{cC} from that shown in panel a. Panel c shows observed hydraulic heads at nest 5-4. Panel d shows the calculated hydraulic head. Numbers represent depths from the ground surface.

Data for the rainfall and runoff were obtained through the courtesy of Dr. Suzanne P. Anderson. Panel c shows a scan of Figure 18 presented by Ebel *et al.* (2007).

shown in Fig. 7 and Table 2, are approximated to the functional relationship used by Ebel et al. (2007) in applying the 3-D model to the results for CB1.

IV. Model application results

Since the VZ model ignores the runoff conversion process of temporal variations between rainfall intensity and runoff rate in the downslope system (Fig. 3), the examination of the model application results begins with an artificial rainfall experiment on a small slope in KI (KIEX), where the distance of the downslope system is very short, the bedrock is impermeable, and the effect of the downslope system can be assumed to be small. The model is next applied to a sprinkling experiment (MREX) on MR, where the existence of rapid flow through bedrock fractures has been demonstrated and to a large rainfall event (MR1) involving two zero-order catchments. After then, the model is extended to events at Kiryu (KI) and Tatsunokuchi-yama (TY), which consist of many slopes and a short stream network. The applications are made for TY first, where most of the rainfall is allocated to storm runoff and the formation of a CAP is clear, and for KI finally, where only about half of the rainfall is allocated to storm runoff due to infiltration into bedrock and a CAP is not reached.

1. Application to small slopes in KI and zero-order catchments in MR

The artificial rainfall experiment (KIEX) on the small slope Plot 2 in KI was conducted eight times at various rainfall intensities (Ohta et al., 1983). Here we use the data from one experiment with strong and time-varying rainfall intensity. Because the site was small and the distribution of soil layer thickness was small, we did not use a semi-infinite length soil column as shown in Fig. 3(2), which is standard in the VZ model applications, but we calculated the flow rate drained from the bottom of a 50 cm soil column with the boundary condition of pressure head ψ fixed at 0.

As shown in Fig. 12, the calculated runoff rate using the soil physical properties of KI in Table 2 well simulated the observed result before and during the CAP and in the recession period. Since the size of the downslope system is only 3 m and the saturated hydraulic conductivity of the sandy soil is large, it can be easily understood that the drainage rate from the bottom of the soil layer caused by the vertical system was almost directly observed as the runoff rate. Therefore, this result confirms the findings of Ohta et al. (1983) that rapid vertical propagation of pressure head caused storm runoff response.

For the application of the VZ model to MREX, the results of Schmidt's (1999) survey of soil

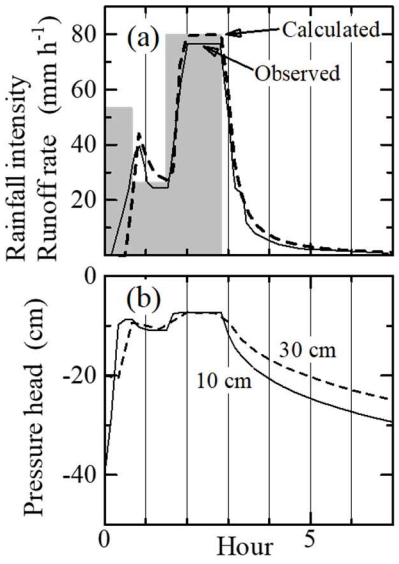

Fig. 12. Comparison of the runoff rate calculated using the VZ model with observed data for an artificial rainfall experiment on a small hillslope in KI.

Panel a shows the observed rainfall intensities and observed and calculated runoff rates. Panel b shows calculated pressure heads. Numbers represent depths from the ground surface.

Panel b shows a scan of Figure 7 presented by Ohta et al. (1983).

layer thickness distribution (hereinafter referred to as the "survey distribution") were used. In addition, the assumption that the thickness of the soil layer was distributed at the same rate up to a maximum value (hereafter referred to as "linear distribution") was also used to compare the calculated runoff rates. The maximum thickness in the latter case was set at 200 cm, based on the results of the former study. Specifically, the thickness increments were 2.5 cm, so the soil layer in the catchment was divided into 81 (=200/2.5+1) layers, and in the calculation step as shown in Fig. 3(2), the runoff rate was obtained by adding up all the downward fluxes of the vertical soil column from the 0 cm depth (where the rainfall would runoff directly) to the 200 cm depth and divided by 81. Two different methods were used to check the sensitivity of the soil thickness distribution to the storm runoff response. In other words, when the VZ model is applied to a catchment storm runoff response, soil layer thickness studies are not available in most cases, so this comparison is meaningful for estimating the runoff response from limited information.

Since the pressure head in the unsaturated zone is also observed in MREX, the observed hydraulic head (sum of the pressure and potential heads) at the nest 5-4 point shown in Fig. 11(c) (Ebel et al., 2007) was also used for comparison with the model calculation. The initial condition was a constant

pressure head value ψ = -100 cm in the entire soil layer, based on the observation results at this plot. The observed hydraulic head is indicated in terms of elevation, but since the elevation of the ground surface could not be read from the paper, the calculated hydraulic head is plotted with the ground surface as the zero criterion in Fig.11(d). Therefore, the observed and calculated values themselves cannot be compared, but the temporal changes can be.

The average rainfall intensity of MREX aas 1.65 mm h^{-1}, but as mentioned earlier, there were diurnal variations even during the steady state period, and the losses described in Section III.3 were continuously generated. Therefore, the downward flux, which was calculated using the surface boundary condition determined by subtracting 20% of the rainfall intensity as evapotranspiration, was regarded as the drainage rate from the bottom of each soil layer, and the flow rate subtracting 0.3 mm h^{-1} infiltrating to deeper layer from the drainage rate was given to the downslope system.

As shown in Fig. 11(b), observed runoff rates, namely, the Q_U at the upper weir and the Q_L at the lower weir, were almost the same, so each calculated runoff rate was assumed to be half of the flow rate integrated over the entire catchment. Since two different methods were used for estimating the distribution of the soil layer thickness as described earlier, the both calculated runoff rates were plotted as Q_{cD} for the survey distribution and Q_{cC} for the linear distribution.

Comparing the observed hydraulic head in Fig. 11(c) and that calculated in Fig. 11(d), we can see that the process of the wetting front progressing to the depth, the time point where the steady state was reached on May 29, and the tendency of the pressure-head propagation to the depth with almost no delay were all well simulated by the VZ model, demonstrating that the Richards equation could be used to explain the vertical unsaturated flow. Fig. 11(b) shows that there is almost no difference between Q_{cD} and Q_{cC}, that the sensitivities of the soil layer thickness distribution are small, and that the calculated runoff rate simulates the increases in Q_U and Q_L up to May 30 and the observed results in the steady state after then. The reason why the calculated runoff rate reaches the steady state about one day later than the calculated hydraulic head in Fig. 11(d) is explained by the fact that the runoff calculation includes drainage from the thicker soil layers from 1m to 2m.

However, during the steady-state period, the calculated runoff rate clearly has smaller diurnal amplitudes than the those observed (see Fig. 11(b), which magnifies the change in runoff rate). As can be seen by comparing Fig. 11(c) and Fig. 11(d), the daily variation of the calculated values tends to be smaller than the observed values also for the pressure head. As described in III.3, the calculations assume that 20% of the rainfall intensity is lost through evapotranspiration at all times during the day and night, but in reality, evapotranspiration should be large during the day and very small during the night. Therefore, the amplitude of the diurnal variation of the calculated values of both pressure head and runoff rate should have been smaller than that of the observed values. Considering the problem in understanding the rainfall input conditions, which is difficult to avoid in experiments using sprinklers, we judged that the observed and calculated values were roughly satisfactory because the timing of the maximum around 9:00 and the minimum around 21:00 were the same, rather than the amplitude of the diurnal fluctuation. Accordingly, the application of the VZ model to MREX suggests that the runoff conversion process is caused by the propagation of pressure head in the vertical system, that the runoff response can be quantitatively explained by the combination of soil physical properties and soil layer thickness, and that the runoff conversion process in the downslope system is negligibly small due to rapid groundwater flow through the fractures.

Next, Fig. 13 shows the results of the application to a large natural rainfall event MR1. The rainfall began around November 12, 1996, and in the event with a total rainfall of approximately 340 mm (total rainfall values were taken from Fig. 3 of Montgomery et al. (2009)), about one hour after the peak runoff rate was recorded by an intense rainfall of 7 mm in 10 minutes, a debris flow triggered by a landslide in a concave area of the lower part of the CB1 catchment occurred between 19:50 and 20:00 on the 18th (Montgomery et al., 2009). Two weirs were destroyed by the debris flow, so Fig. 13 shows the observed runoff rate up to that point is shown in Fig. 13.

The initial conditions required for model calculations are the same as for MREX, but considering that MREX was in early summer and MR1 was in late fall, and considering the local climatic conditions with low summer rainfall, it is unlikely that the initial conditions will be on the drier side than this assumption. Therefore, although there is a possibility that calculated values may be lower than observed values in the early part of the event, the effect of the initial conditions will be negligible in the latter part of the event. The 20% evapotranspiration subtracted from the rainfall in MREX was not adopted because it is a special case of localized sprinkler water given only in the CB1 catchment, and only the 0.3 mm h^{-1} deep infiltration rate was subtracted from the drainage rate at the soil-layer bottom.

As mentioned earlier, because of the uncertainty issues associated with the lower weir runoff Q_L, both the upper weir runoff Q_L and Q_U are expressed in units of L s^{-1} rather than mm h^{-1}, i.e., runoff per unit catchment area. (Fig.13(b)). The Q_U is the discharge from the soil layer of CB1, whose catchment area is

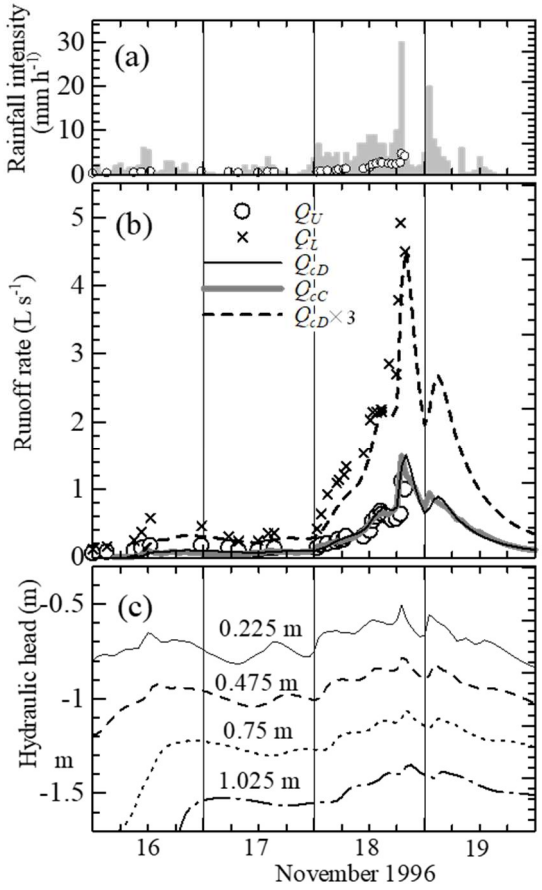

Fig. 13. Comparison of calculated runoff rate by the VZ model with that observed for the storm of November 1996 (MR1) in MR when a landslide was initiated in CB1.

Panel a shows observed rainfall intensity and runoff rate from the upper weir. Panel b shows observed and calculated runoff rates. Q_U, Q_L, Q_{cD}, and Q_{cC} are the same as those in Fig. 11. Panel c shows the calculated hydraulic heads. Numbers represent depths from the ground surface.
Observed rainfall and runoff show scans of Figures 3 and 9 presented by Montgomery *et al.* (2009).

known as 860 $m^{2,}$ can be converted into the unit of mm h^{-1}. However, the Q_L is the discharge from a catchment composed of CB1 and its western neighbor, the entire catchment area of which is unknown. In addition, the discharge from the soil layer was designed not to pass through the lower weir. For these two reasons, it is not possible to convert Q_L values into the unit of mm h^{-1}. The Q_U is shown mm h^{-1} in Fig. 13(a), which indicates that the quantitative relationship between Q_U and rainfall for the upper weir is almost the same as that for the MREX shown in Fig. 11(a).

Based on these characteristics of the observation design, we determined the following method of calculated runoff for comparison with Q_L. First, as with MREX, it was assumed that 1/2 of each of the runoff rates obtained by the VZ model was allocated to the upper and lower weirs to get the runoff rate in the unit of mm h^{-1}. Since the upper weir measured discharge from the soil layer in the CB1 catchment only, the calculated runoff rate for the upper weir in units of L s^{-1} was multiplied by the area of the watershed, 860 m^2. For the lower weir, the area of the catchment is estimated to be about three times larger than that of CB1, so the calculated runoff rate in the unit of mm h^{-1} was converted to that in the unit of L s^{-1}, assuming that the area is three times larger (2580 m^2). This approach implies that the distribution of soil thickness, that of soil physical properties, discharge from the soil layer, and exfiltrating from the 15 m channel bed between the upper and lower weirs are all assumed to be the same between CB1 and the other catchment of the lower weir.

Fig. 13(b) shows that the VZ model results generally simulate the observed runoff rates (Q_U and Q_L) until the measurement was interrupted by the occurrence of debris flow, even during natural rainfall. For the upper weir, calculation results by the two types of soil layer distributions are plotted, Q_{cD} from the survey distribution and Q_{cC} from the linear distribution, both of which simulate the observed Q_U, suggesting that, as in MREX, their sensitivity to the runoff conversion process is small. For the lower weir, the temporal variation of runoff rate is well simulated, albeit with some uncertainties. Therefore, the assumption of the VZ model that the runoff conversion process is mainly controlled by the vertical system, as explained for the case of MREX, can be assumed to be applicable to a large-scale rainfall event such as MR1, until just before the debris flow occurrence.

Fig. 13(c) shows the calculated hydraulic head. The downward development of wetting front from the ground surface to the deeper part of the soil layer during Nov. 16, when the soil is not sufficiently wet, is similar to the period before reaching the steady period in MREX. (Fig. 11). In addition, as shown in the steady state in MREX, a rapid vertical propagation is detected in the pressure head distribution just during a CWC before the debris flow occurrence. Observation has recorded a sharp increase in pore pressure around the bottom of the soil layer and the weathered bedrock immediately after heavy rainfall, and this observation phenomena may be simulated by the calculations.

These results indicate that, in large rainfall events, the temporal variation of rainfall is quickly transmitted to the deeper soil layers when intense rainfall occurs after the soil layer becomes CWC, and that even if the debris flow occurrence, the runoff mechanism driven by vertical flow controls the runoff conversion process until just before the occurrence. Based on these results, we will discuss the relationship between storm runoff and the occurrence of landslide in Section V.2.

2. Application to TY

First, the VZ model was applied to the observation results of TY1, which were also treated by Tani et al. (2020), and the results are shown in Fig. 14. In SL, a valley-side slope, pressure head observations were obtained at the points shown in Fig. 5, and these are shown together with the calculated values from the VZ model. The initial condition was ψ = -400 cm at all

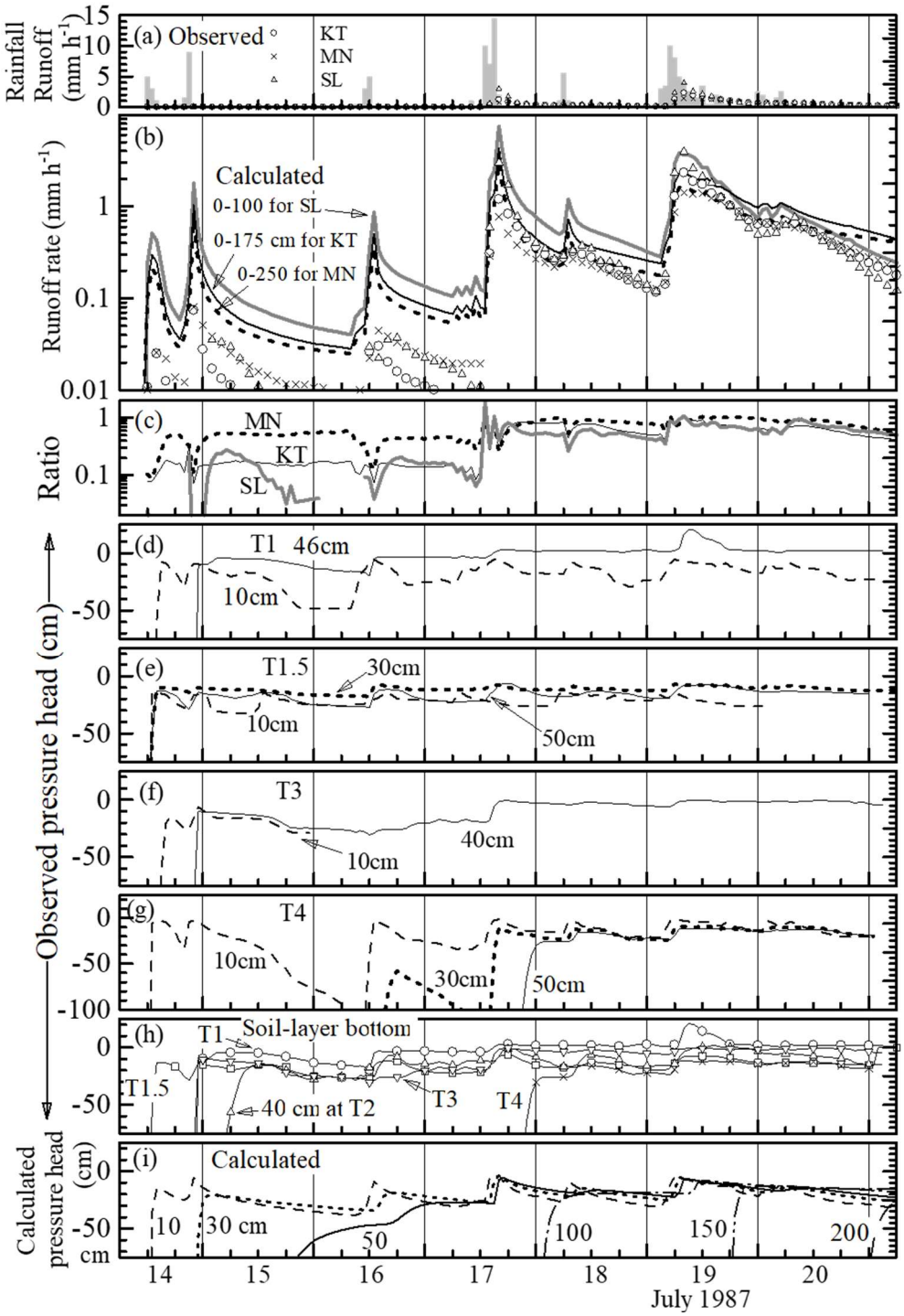

Fig. 14. Comparison of the runoff rate calculated using the VZ model with that observed for a storm in August 1988 (TY1) in KT, MN, and SL in TY.

Panel a shows the observed rainfall intensity and runoff rates. Panel b shows the observed and calculated runoff rates. Panel c shows ratios of observed runoff rate to that calculated. Panels d–g show observed pressure heads. Panel h shows the pressure head values at the deepest point of each observation site. Panel i shows the calculated pressure heads. Numbers represent depths from the ground surface.

depths based on the observations at SL. In TY, the distribution of soil layer thickness over the entire catchment has not been investigated. Therefore, we adopted a linear distribution based on the fact that the calculated runoff rate by this method was almost the same as that by the survey distribution for MR (Fig. 11(b) and Fig. 13(b)). The maximum value of the linear distribution of the soil layer thickness was determined through a trial and error method, so that the calculated hydrographs might match those observed, after July 19 when the soil reached CWC. The maximum values of 100 cm for SL, 175 cm for KT, and 250 cm for MN were obtained as good results. Calculations for TY2 was made with the same parameters and initial conditions as TY1, and the results were compared with the observed values (Fig. 15).

For both TY1 and TY2, the calculated runoff rates were higher than those observed in the early stage, and the calculated and observe values gradually agreed with each other (Fig. 14(b) and Fig. 15(b)). For TY1, the ratio of calculated runoff rate to that observed (hereinafter referred to as the ratio of runoff rate) in Fig. 14(c) shows that the ratio was less than 1 until the subevent on July 17. The reason for this is that the thin soil layers in the watershed are isolated from each other and do not become a contribution area to the storm runoff, as shown in step (1) in Fig. 2. The ratio of runoff rate is also increasing in TY2 by the sub-event on Sep. 10, reflecting the expansion process of the contribution area from isolation to combination. The ratio approaches 1 after the sub-event on Jul. 17 in TY1 and that on Sep. 10 in TY2, and this value of 1 means that the CWC in the calculation becomes connected each other as the contribution area, so this period is considered to correspond to step (2) in Fig. 2.

The calculated pressure heads of TY1 and TY2 are plotted in Figs. 14(i) and 15(d), respectively, and the model calculation results show that the pressure head rises to near zero and the CWC gradually extends into the thicker soil layer. The calculated pressure head is reflected in the calculated runoff rate, which matches those observed after Jul. 19 for TY1 and the Sep. 11 for TY2. However, as shown in Fig. 15(d), in TY2, even in MN with a soil layer maximum of 250 cm, the soil layer

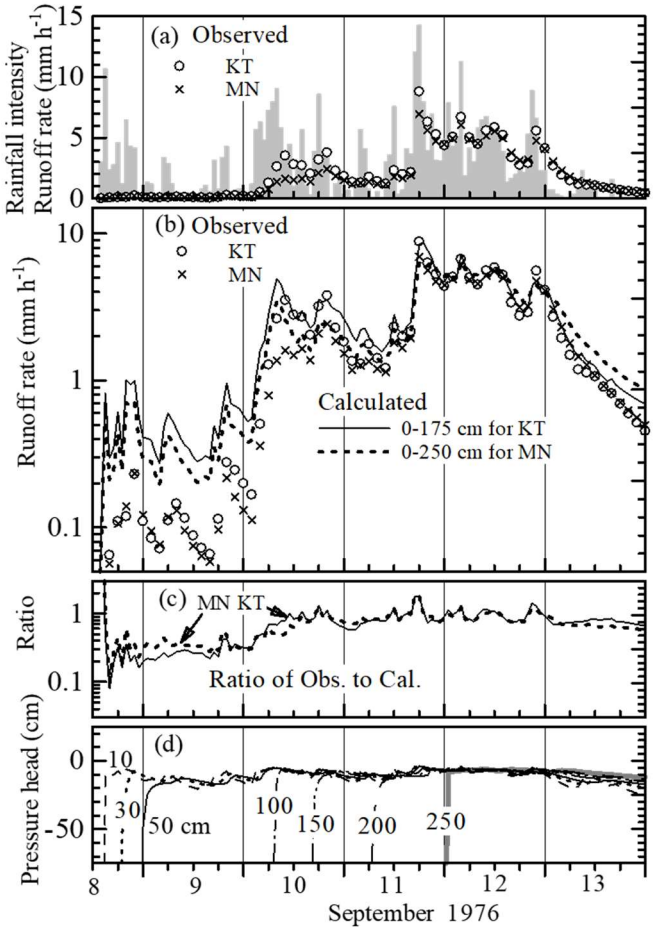

Fig. 15. Comparison of the runoff rate calculated using the VZ model with that observed for a storm in September 1976 (TY2) in KT and MN in TY.

Panel a shows the observed rainfall intensity and runoff rates. Panel b presents the observed and calculated runoff rates. Panel c shows ratios of the observed runoff rate to that calculated. Panel d shows the calculated pressure heads. Numbers represent depths from the ground surface.

in the entire catchment reaches the CWC after the rainfall on Sep. 11, while in TY1, where the rainfall magnitude is smaller, it does not (Fig. 14(i)). The correspondence between the CWC and the expansion of the runoff contribution area is discussed in more detail in V.1 for TY1 where the observed pressure head is available.

3. Application to KI

In applying the VZ model to KI, both the survey distribution and the linear distribution were used for the distribution of soil layer thickness, as in MR. In the latter method, the mean thickness of 65 cm was used as the median value up to a maximum value of 130 cm, since the area occupied by the thick soil layer of the riparian was negligible. In addition, with reference to the storm runoff distribution characteristics of rainfall shown in Fig. 9, it was assumed in the calculations that one half of the drainage rate from the bottom of the soil layer was distributed between the inflow into the downslope system and the deep percolation into the weathered bedrock. For the initial conditions, ψ = -100 cm was used for KI2, based on the observation by Katsura et al. (2014), while the same value as for KI2 was applied for KI1, for which no information was available.

Figs. 16 and 17 compare the calculated values with those observed for KI1 and KI2, respectively. Regarding the influence of the method for the soil-layer thickness distribution, the calculated values based on the survey distribution (Q_{cD}) and those based on the linear distribution (Q_{cC}) are almost identical, and the sensitivities are small for both events.

Since the observed initial runoff rate before the event for KI1 was smaller than that for KI2, the initial condition of KI1 was estimated to be on the drier than that of KI2, i.e., ψ < -100 cm, and if the initial condition was given more correctly, the calculated runoff intensity of KI1 in the early stage of the event would be smaller. However, the calculated values for the initial phase of KI1 did not deviate much from the observed values as in KI2 (Fig. 16(b) and Fig. 17(b)). Therefore, the effect of the initial soil moisture condition is considered small.

The tendency that the calculated runoff rate is larger than that observed until the soil layer reaches CWC is resolved around 9:00 on Aug. 1 in the case of KI1 and around 12:00 on July 18 in the case of KI2. Therefore, it can be inferred that the distribution of rainfall to runoff increases with cumulative rainfall in KI as well, although more slowly than in TY, and that the CWC is gradually connected, resulting in the expansion of the contributing area as shown in Fig. 2(2). Nevertheless, to simulate the observed runoff rate well, one half of the drainage rate from the soil-layer bottom must be treated as deep infiltration, which is a major characteristic of KI that differs from TY.

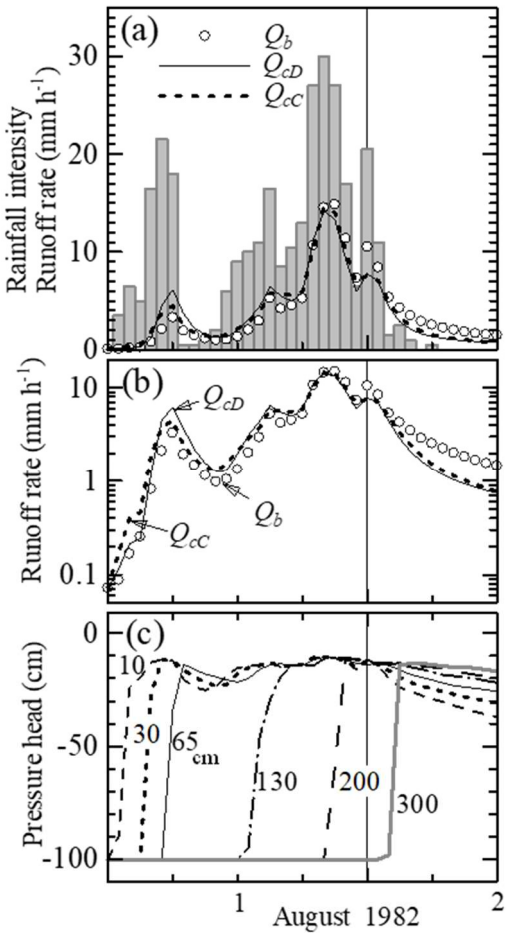

Fig. 16. Comparison of the runoff rate calculated using the VZ model with that observed for a storm in August 1982 (KI1) in KI.

Panel a shows observed rainfall intensities and observed and calculated runoff rates. Panel b shows the observed and calculated runoff rates. Q_b, is the observed runoff rate. $Q_{cD,}$ and Q_{cC} respectively denote the observed runoff rates calculated using the investigated and linear distributions of soil-layer depth. Panel c shows the calculated pressure heads. Numbers represent depths from the ground surface.

After the point when both KI1 and KI2 become CWC, the calculated values can simulate those observed well. The calculated pressure head in Figs. 16(c) and 17(c) shows that the pressure hydraulic head rises near zero values down to a depth of 130 cm, which is set as the maximum thickness of the soil layer, indicating that almost the entire catchment reaches CRC. Therefore, even when the soil layer of the entire catchment becomes CWC, it does not reach a CAP for KI unlike for TY, and the allocation ratio of rainfall to flow in the downslope system does not seem to increase beyond 1/2. The runoff mechanism of KI will be discussed in detail in Section V.4.

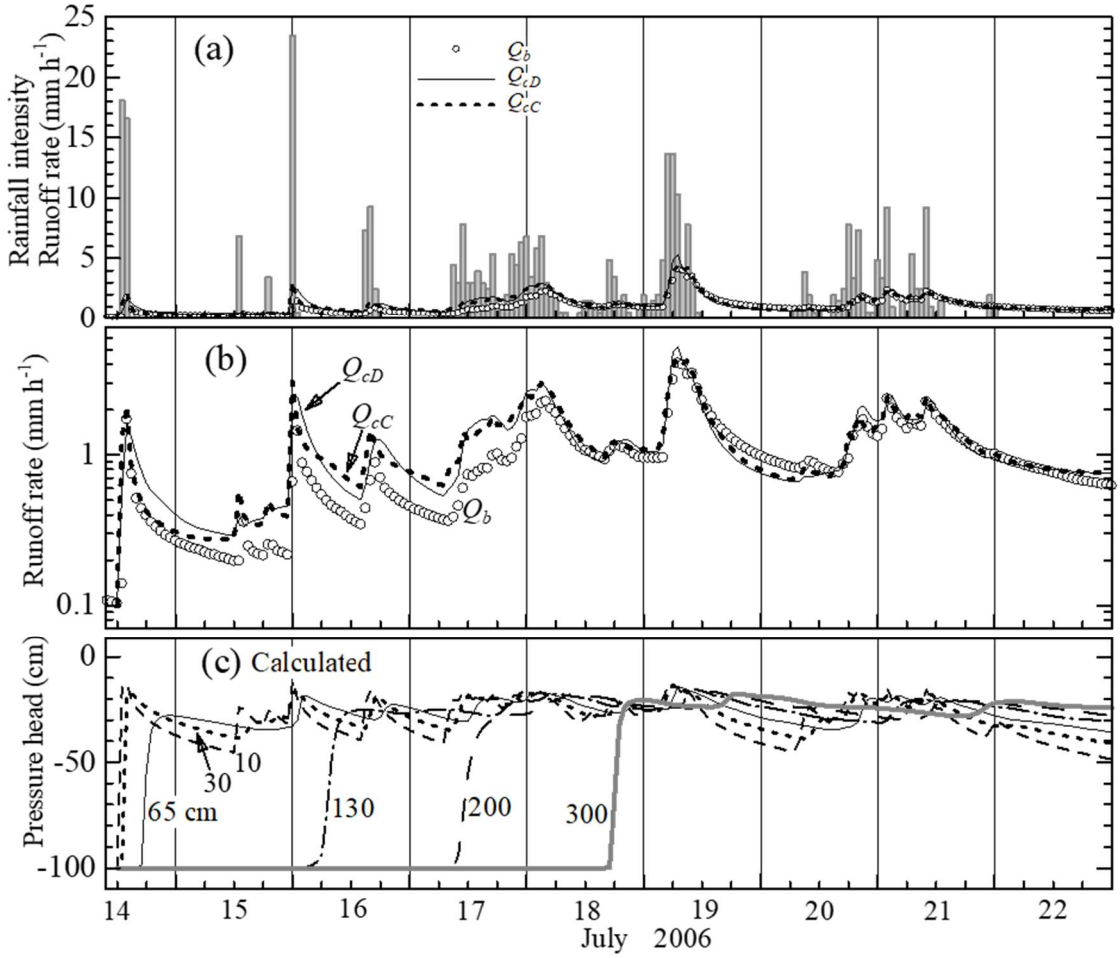

Fig. 17. Comparison of the runoff rate calculated using the VZ model with that observed for a storm in July 2006 (KI2) in KI.

Symbols are the same as those in Fig. 16.

V. Discussion on runoff mechanism

In this paper, based on the "concept emphasizing the role of the vertical system on storm runoff response" proposed by Tani et al. (2020), a runoff model was developed and applied to small mountainous catchments with good results. This VZ model differs significantly from conventional physically-based runoff models, in which the runoff conversion process of temporal variations between rainfall intensity and runoff rate is based on the downslope system. This chapter discusses the runoff mechanism from several viewpoints derived from on the results of the VZ model application.

1. Runoff mechanism related to the variable contribution area

The VZ model assumes that all drainage from the bottom of the soil layer, which is obtained from the calculation of vertical unsaturated flow in the CWC, contributes to the runoff. In practice, however, the contribution does not occur when the CWC is spatially isolated, as shown in Fig. 2(1). Therefore, we will discuss the runoff mechanism in the process of interconnection of CWC areas and their expansion to become the contribution areas by comparing the observed values in TY1 with those calculated.

Figure 14(h) summarizes observed values of the pressure head ψ near the bottom of the soil layer at SL. The observed ψ values at the lower part of the slope, except T4, increase to near zero in response to the rainfall on Jul. 14, but this wetting process seems to be affected by the local spatial heterogeneities in each observation point, such as the heterogeneity of soil physical properties and the presence of preferential pathways, as seen in time differences between the earliness for T1.5 and the lateness for T2.

Figure 14(b) shows that after the rainfall on the Jul. 16, the observed and calculated SL runoff rates are almost parallel. This means that the ratio of runoff rate remains constant in Fig. 14(c), but that the value is still around 0.2. In the calculation, the CWC

area extends with time according to the assumed linear distribution of soil layer thickness, so the fact that the runoff rates are parallel and the ratio of runoff rate is constant suggests that the observed and calculated contribution areas extend in parallel, even if the observed contribution area is smaller than the calculated CWC area. However, the ratio of 0.2 suggests that the CWC area is not connected to the lower edge of the slope, even if the area occurs in the thin soil layer above the mid-slope (bedrock is exposed in some area on the slope). Therefore, it is inferred that the expansion of the contribution area is limited to the stage shown in Fig. 2(1), and is restricted to a narrow area at the bottom of the slope. The observation result shown in Fig. 14(g) that ψ at the depth of 50 cm at T4 in the mid-slope rises for the first time after the rainfall on Jul. 14 also supports this suggestion.

The ratio of runoff rate for SL exceeded 0.5 due to rainfall on Jul. 17, indicating that a large amount of rainfall may combine isolated CWC areas each other and expand the contribution area. The maximum value of the SL soil layer is set at 100 cm in the calculation, and the calculated value of ψ at that depth increases to nearly zero on Jul. 18 (Fig. 14(i)), indicating that the CWC has expanded over the entire SL catchment area and reached the stage shown in Fig. 2(iii). The ratio of runoff rate reaches 1 at the beginning of the rainfall on Jul. 19, which indicates that most of the catchment area actually reaches the contribution area and the CAP is completed for SL.

Looking at the relationship between cumulative rainfall and cumulative storm runoff in Fig. 6, MN and KT have larger cumulative runoff than SL up to about 70 mm cumulative rainfall, while SL is almost zero. Oppositely, SL has the largest total runoff of this event, followed by KT and MN (Table 1). This trend is shown in the relationship between total rainfall and total storm runoff also in other rainfall events: SL has smaller total runoff than the other two catchments up to a total rainfall of about 70 mm in general, but SL increases more rapidly as the total rainfall increases.

The ratios of runoff rate for KT and MN shown in Fig. 14(c) become stable earlier than the ratio for SL due to rainfall on Jul. 14, and approach 1 after the rainfall on Jul. 17. This suggests that the CWC areas in KT and MN are gradually connected by rainfall, and that the areas expand in the stage shown in Fig. 2(2) after Jul. 17, overlapping with the contribution areas. After that, the calculated runoff rate simulates that observed well in response to rainfall on Jul. 19. However, the ψ values calculated by the VZ model in Fig. 14(i) show that the depth at which ψ increases to near zero is up to 100 cm after the rainfall on Jul. 17 and up to 150 cm after the rainfall on Jul. 19. Therefore, it can be inferred that the responses to the rainfall on Jul. 19 for KT, where the maximum thickness of the soil layer is 175 cm, and for MN, where the maximum thickness is 250 cm, are still in the stage shown in Fig. 2(2) because the thick soil layer remains dry within the catchment area and does not reach the CAP.

The difference between SL and KT and MN can be explained in terms of soil layer and topography: SL is a valley-side slope with no concave zones and does not include areas with thick soil layers, while KT and MN are catchments that include river channels and have a wide distribution range, including areas with thick soil layers. Therefore, CWC areas along concave zones such as hollows and stream channels easily combine each other as shown in Fig. 2(2), and storm runoff tends to increase even during periods of small cumulative rainfall. On the other hand, it is presumed that the CAP in Fig. 2(3) is reached later in a catchment than that in SL because the thick soil layer does not become CWC even if the cumulative rainfall becomes large.

2. Runoff mechanism derived from landslide occurrence

In IV.1, the VZ model was applied to a rainfall event MR1 that caused the landslide occurrence. It was inferred that the runoff mechanism, which was mainly based on the runoff conversion process in the vertical system assumed in the model, was sustained until immediately before the occurrence. Montgomery et al.'s (2009) study of the MR1 event showed that a rapid increase in pore pressure near the lowest portion of the soil layer and in the fracture-rich weathered bedrock was recorded immediately after a heavy rainfall event. The study of the site of the landslide showed that the ratio of pore water pressure to soil thickness immediately before the landslide was locally larger in the fractured areas than in the surrounding areas. These results suggest that the localized increase in pore pressure is the cause of the landslide. A result of the hypothetical runoff rate obtained by applying the VZ model to the observed rainfall after the occurrence of the landslide, as shown in Fig. 13(b), suggest that the runoff mechanism in the absence of a landslide can be explained as a combination of vertical flow and downslope flow in the fracture, and that the landslide may have occurred when water is forced into the soil layer beyond the limits of the fracture's drainage capacity due to increased pore pressure. We will have a further discussion the mechanism of runoff during heavy rainfall events that may lead to landslide, referring to previous studies.

Tani (1982; 1985a; 1985b) clarified the characteristics of vertical unsaturated flow when the bottom boundary condition is impermeable at an early time when numerical calculations using the Richards equation were scarce. In other words, when the volumetric water content was already close to the saturated water content and there are few pore spaces

left empty, the groundwater level rose rapidly and significantly in response to an intense rainfall. Therefore, the explanation for MR1 that "during the period when downslope drainage through fractures reached its limit and exfiltration from the fractures into the soil layer was occurring, the landslide occurred immediately due to a rapid increase in pore pressure caused by an intense rainfall" is reasonable in view of the vertical unsaturated flow process.

If the soil layer is destroyed due to a landslide occurrence, the space for the runoff mechanism itself must disappear, and the runoff characteristics will change dramatically from that moment on. However, even if landslide does not occur, for example, but when the groundwater table rises to the soil surface and saturation excess overland flow is generated, the runoff mechanism is expected to change qualitatively and affect the runoff response. The VZ model assumes that the effect of downslope system on the runoff conversion process is negligible due to a rapid drainage through preferential pathways, but an application of the model may not be satisfied when the groundwater table rises beyond the limit of drainage capacity in practice. Although such qualitative changes in the runoff mechanism may appear when the rainfall magnitude increases, in the actual data, the runoff rates calculated by the VZ model, which did not take such changes into account, well explained the observed rates until just before the landslide occurrence, as shown in Fig. 13(b). This result suggests that the qualitative change of the runoff mechanism producing the runoff conversion process was not generated just before the soil layer was destroyed by the landslide.

From the above application of the VZ model to MR1, it can be inferred that the vertical-dominated runoff mechanism might have been maintained unless the runoff space was eliminated by a landslide occurrence. In general, whether or not a landslide will occur is governed by an uncertainty and is difficult to determine from rainfall conditions. However, if the soil layer achieves a CWC due to sufficient cumulative rainfall, a landslide is likely to occur. It is plausible that the probability of landslide occurrence increases as the degree to which the drainage capacity of the downslope system is exceeded.

In fact, studies on evacuation Cs for mountain hazards in Japan empirically showed that landslides often occurred immediately after strong rainfall events following an increase in cumulative rainfall (Suzuki et al., 1979; Senoo et al., 1985; Kikui and Senoo, 2004). Based on this knowledge, the Japan Meteorological Agency (JMA) has developed a soil rainfall index and applied it to evacuation advisories, and this index is utilized in disaster prevention work by local governments (Okada, 2002; 2016). However, the mechanism of why the combination of cumulative rainfall and intense rainfall causes a landslide occurrence has not yet been fully explained, although it was mentioned that increased pore pressure was involved (Danjo, 2017; Liu et al., 2022).

In this problem, if the runoff mechanism assumed by the VZ model is taken into account, it can be rationally explained that if there is an intense rainfall after the soil layer is in the CWC by sufficient cumulative rainfall, the rapid runoff conversion process in the vertical system increases the discharge rate from the soil layer into the downslope system, causing a rapid increase in pore pressure beyond the limit of the drainage capacity in the downslope direction. This explanation can be used to understand the relationship between rainfall condition and the landslide occurrence.

From the above discussion, it can be inferred that the occurrence of landslide depends on the limit of drainage capacity in the downslope system. However, considering an empirical fact that soil layer collapse occurs only once in a period of several hundred years or more (Kaki, 1958; Iida, 2012; Uemura et al., 2022), the drainage capacity of the downslope system must be considered quite large. In conclusion of this section, I would like to propose the hypothesis that "the reason why storm runoff response is mainly dominated by the vertical system rather than the downslope system is that the capacity of the downslope system to quickly drain groundwater from the soil layer under a CWC is large enough to keep the soil layer stable without landslides for more than several hundred years", although it may be a bold statement to say so.

3. Runoff mechanism in the bedrock producing storm runoff response

In MR, fractures near the surface of weathered bedrock have been detected as an important pathway in the downslope system that generates storm runoff responses, and this mechanism has been noted elsewhere (Onda et al., 2001). Therefore, we would like to consider the mechanism by which the thick weathered bedrock of Paleozoic Formation in TY can produce storm runoff responses. For this discussion, Hosoda and Tani (2016) conducted observations in the upper and middle part of the ZC slope (Fig. 4) of the pressure head of the soil layer (vertical distribution up to 160 cm in the upper part of the slope and 320 cm in the middle part) and the groundwater level in boreholes penetrated into the weathered bedrock (till 10.5 m depth in the upper part of the slope and 17.5 m deep in the middle part).

In KT and MN of TY, when cumulative rainfall is large, the CWC area expands to the entire catchment and a CAP is established. According to Hosoda and Tani (2016), the groundwater level in the bedrock shows rapid fluctuations similar to the storm runoff response when the soil layer becomes CWC. Considering this information together, it can be inferred

that the runoff conversion process producing storm runoff responses is generated by the vertical system, causing rapid fluctuations in groundwater levels, which are directly transmitted to the temporal changes of runoff rate through flow paths included in the downslope system. This presumption implies that the drainage capacity of the downslope system is high enough. According to Hosoda and Tani (2016), the estimated saturated hydraulic conductivity based on the straight-line technique of the transient method (Japanese Geotechnical Society, 2004) during a rainfall period when the water level in the borehole in the middle of the slope rose considerably was about 3.8×10^{-3} cm s^{-1}, 100 to 1000 times greater than the value obtained from the field hydraulic tests conducted in the dry winter season. Although information is still scarce, it must be considered that the runoff of a downslope system in the bedrock has mechanisms that can contribute to rapid storm runoff responses.

Unlike the MR case, in the TY case, no path information such as fractures is available, so the mechanism of the downslope system can only be estimated indirectly. First, during the CWC, when the pressure head of the soil layer rises to near zero till deep zones, the runoff conversion process occurs mainly in the vertical system, as repeatedly mentioned. Since the total storm runoff is almost equal to the total rainfall in a CAP, the contribution area must be considered to extend over the entire catchment, as shown in Fig. 2(3). Based on field observations during rainfall events, overland flow does not occur except along river channels and trails of man and beast, so it should be assumed that the drainage pathways are located in the subsurface structure. Although it is difficult to determine the depth, it is assumed that somewhere within the subsurface structure, from the soil surface to the weathered bedrock, a change of water flow from the vertical direction to the downslope occurs, and a downslope system with high drainage capacity that extends over the entire catchment from ridge to valley must produce the runoff conversion process contributing storm runoff responses in the stream channel. Such a runoff mechanism is not inconsistent with the assumption of the VZ model that occurs predominantly in the vertical system, while the downslope system transmits the waveform as it is.

The above considerations can point out a major difference in the information on runoff mechanisms in vertical and downslope systems. Information on the actual state of the vertical system can be provided by observations on the propagation of the pressure head in SL and on the fluctuation of the borehole water level in ZC, and even though the water retention and permeability characteristics of the weathered bedrock are not easily estimated, it is possible to simulate the runoff conversion process there using the Richards equation. On the other hand, even if it can be inferred that the rapid drainage of a downslope system is caused by a network of longitudinally and vertically distributed fractures, no information on their distribution structure or hydraulic properties is usually available. We are forced to recognize the difficulty of understanding the mechanism of the downslope system. Notwithstanding, by analyzing the results of field observations using the VZ model, we have been able to identify that the issues that need to be studied in the future are the spatial distribution and hydraulic characteristics of flow pathways within the weathered bedrock contributing to in the downslope flow system. This is regarded as the conclusion of our discussion in this section.

4.Runoff mechanisms in deeply-weathered granite catchments

As Shimizu (1980) and Musiake et al. (1981) have already shown, the flow regime of mountain rivers in Japan greatly depends on the geology: rivers flowing from sedimentary rock catchments tend to have larger stormflow and smaller baseflow than those from catchments of other geology, and the total storm flow there generally approaches the total rainfall as the storm magnitude increases (Tani et al., 2012).

In contrast, granite mountainous catchments, including KI, have more stable flow regimes and higher base flow than sedimentary rock catchments. The saturated hydraulic conductivity of the bedrock in the granite catchments, where the rocks are deeply weathered, is relatively high with a value of about 1×10^{-4} cm s^{-1} measured at WS within the KI catchment (Katsura et al., 2006). The rock mass, except for the core stones, is strongly weathered into a permeable medium called "masa," which looks as if it were sandy soil. Therefore, even if the fluctuation of water level is the same, the fluctuation of storage volume included in the weathered granite bedrock is much larger than that in a bedrock with fractures as shown in the sedimentary rock mountains. As a result, the granite bedrock may act like a huge dam reservoir, producing with stable flow regimes with high baseflow (Musiake, 1982; Tani et al., 2012).

Differences in runoff response characteristics by geology had a significant impact on the results of the VZ model application. In the sedimentary rock catchments, TY and MR, the entire of each could be considered to reach a CAP with a CWC. Both TY and MR contain fractures in the bedrock, but the bedrock outside of the fractures may not be functioning as the permeable medium that produces large fluctuations of water storage. On the other hand, in a granite catchment KI, one half of the rainfall is stored within the weathered bedrock, the large storage fluctuations of which produce a buffering effect, resulting in little storm runoff response from the bedrock even with high

cumulative rainfall. This section examines the mechanism of storm runoff in granite mountainous catchments where storm runoff does not reach the rainfall volume even during large rainfall events, based on our application results of the VZ model that an almost constant percentage of the calculated storm runoff rate was almost identical to that observed.

Katsura et al. (2014) observed the spatial distribution of pressure head through soil layers and weathered bedrock in a zero-order catchment WS within KI, which provided the following important information needed for the discussion here: in the WS, water level observations in boreholes drilled in the bedrock till the lower elevation than the runoff-rate observation weir were made in the upper and middle part of the catchment. According to these observations, the elevation of the groundwater table above sea level from the upper to the lower part of the catchment was similar to each other and tended to fluctuate up and down while remaining nearly horizontal and a reverse gradient was sometimes generated. As a result, there was a thick unsaturated zone in the weathered bedrock in the upper part of the catchment, while the groundwater level was closer to the surface and the unsaturated zone was thinner in the lower part of the catchment. Therefore, when the KI2 rainfall began, the groundwater level within the weathered bedrock in the lower part rose due to the relatively high level prior to the rainfall, and a ridge of the groundwater level (i.e., groundwater level higher on the valley side than on the ridge side) was formed on July 18. As a result, Katsura et al. (2014) stated that the groundwater level in the upper side of the catchment remained deep within the bedrock throughout the rainfall event, allowing deep infiltration to continue and not became a contribution area to runoff, whereas the level in the lower side was shallow enough to intercept infiltration and became a contribution area that produced the storm runoff response (Katsura et al., 2014).

The value of the saturated hydraulic conductivity K_s of the weathered bedrock was mentioned earlier and corresponds to about 3.6 mm h^{-1} in the unit used for rainfall intensity (Katsura et al., 2006). Therefore, taking into account the effect equalizing the temporal variation through the vertical infiltration within the soil layer (Kosugi et al., 2006), it is considered possible that even rainfalls stronger than this value can infiltrate deeply into the weathered bedrock. Consequently, if the groundwater level is sufficiently lower than the surface of the weathered bedrock in the upper part of the catchment near the ridge, flow into the downslope system is unlikely to occur. However, the above K_s value is too small to generate storm runoff through downslope flow within the weathered bedrock even though it allows vertical flux to infiltrate to deep zone of the bedrock, The flow velocity of the fractures in MR, for example, was about 7-15 meters per hour (Anderson et al., 1997), which was much greater than that estimated from the K_s value in WS. Therefore, the hydraulic conductivity of the weathered bedrock, which acts as a permeable medium, is unlikely to produce storm runoff in a downslope system, even if it can produce baseflow. However, the K_s value of the soil layer in KI is 0.19 cm s^{-1}, which corresponds to about 7 meters per hour, as shown in Table 2, reflecting the sandy soil, and is very high. In addition, it is also possible that pipe-like preferential pathways may be naturally developed in concave zones or at the slope bottom, where the storm flow concentrates, to drain it. In fact, the existence of pipes has been confirmed in a zero-order catchment in Fudoji located also in the granite Tanakami Mountains (Uchida et al., 2003). Although the presence of pipes within the soil layer or fractures near the surface of the bedrock was not been detected in WS, it is possible that these preferential pathways might act for generating storm runoff.

Studies have been continued to elucidate the runoff mechanism based on flow and water quality observations in four sub-catchments included in the overall KI catchment (Katsuyama et al., 2005; 2010). A large amount of sediment is deposited in the upstream areas of check dams constructed accompanied with the revegetation work for devastated hillslopes, and riparian zones along stream channels are created in the KI catchment. Stream water during the baseflow period is dominated by components discharging through the bedrock, although it may be affected by seasonal changes in evapotranspiration and have a larger proportion of the components from the soil layer at least in winter (Suzuki, 1984). According to the endmember analysis by Iwasaki et al. (2015), when rainfall began, the proportion of "new water" such as rainwater falling near the stream channel increased and the proportion of “old water” such as soil water and bedrock water decreased. However, the absolute amount of old water itself rather increased. Therefore, the contribution of old water was significant even during the storm runoff period. Old water included not only soil water but also water stored in the bedrock, the latter of which was considered to be exfiltrated from the bedrock surface into the riparian or stream channel (Iwasaki et al., 2015).

Let us recall that such exfiltration from weathered bedrock into the stream channel was also observed at the lower weir in MR. (Anderson et al., 1997). In KI, we may assume that the weathered bedrock not only contains permeable media with K_s of 1×10^{-4}cm s^{-1}, but also pathways composed of more permeable fractures producing storm runoff responses. This is because the permeability of bedrock is formed through long-term geomorphic development and weathering processes, and fractures in the bedrock are also may be developed through these processes

(Kashiwaya and Yoneda, 2004). In a granite mountainous catchment, as described above, after the temporal variation of rainfall intensity is equalized by the vertical system, the variation is quickly transmitted to storm runoff rate in the stream runoff rate through the downslope system in the lower part of the catchment, while stable baseflow rate is recharged through storage fluctuations in the permeable media within the bedrock in the upper part of the catchment. Ultimately, the above runoff mechanisms can be estimated from the studies conducted in KI.

Application of the VZ model to a deeply-weathered granite mountainous catchment has confirmed that the runoff conversion process is mainly explained by the vertical system. However, the observed runoff rates were equivalent to about half of the calculated rates. This fact means that only half of the observed values could be reproduced *by chance*, which strongly suggests that the runoff characteristics of a granite mountainous catchment are not determined only by the vertical system, but can vary depending on the flow of the downslope system within the subsurface structure, including the weathered bedrock. We will now turn to further discussion of this diversity of runoff characteristics and the reasons producing it.

5. Dependence of runoff mechanism on topographic development

In the previous section, it was inferred that the upper part of catchment did not contribute to storm runoff responses because of continuous deep infiltration in the case of a granite mountainous catchment with a deeply-weathered bedrock even when the soil layer was in a CWC. In KI, the distribution ratio of rainfall to storm runoff was estimated to be fairly stable at about 1/2, but a smaller ratio was observed in another catchment. In this section, we discuss the mechanism of runoff that results in different distribution ratios.

Kosugi et al. (2011) conducted detailed hydrological observations, including water level measurements in numerous boreholes drilled in the weathered bedrock in the Nishi'otafuku-Yama Experimental Watershed (NO), which had a catchment area of 2.1 ha near the summit of Rokko mountain range. Their observations showed that the catchment area was roughly divided into upper, middle, and lower parts from the hydrologic point of view, and it was inferred that these divisions were caused by faults in the bedrock associated with mountain uplift. Looking at groundwater fluctuations in detail, temporal changes of the groundwater levels in the upper part of the catchment were not directly reflected by those in the runoff rate discharged from the catchment. However, changes in the levels in the central and lower parts, fluctuations in the level were reflected in those in runoff rate from the catchment. In the middle part, which had a large horizontal extent, an aquifer with very gradual groundwater level fluctuations was widespread, while the bedrock groundwater level in the lower part demonstrated a combination of the fluctuations shown in the middle part and those on original shorter time scales. The groundwater level within the soil layer in the lower part showed a combination of two types of gradual fluctuations, due to supply from the weathered bedrock, and flashy increases and decreases in response to storm runoff. As a result, the runoff rate from the catchment showed a complex temporal variation with three overlapping peaks, reflecting the two types of gradual changes seen in the storm runoff and the groundwater level within the lower bedrock. Hence, the magnitude of storm runoff was much smaller than that for KI because it was only supplied from the lower part of the catchment (Kosugi et al., 2011), and the storm runoff volume appears to be less than 10% of the total runoff volume, based on hydrographs for periods longer than one year.

The Rokko and Tanakami mountain ranges have different histories of landform formations by tectonic uplift (Fujiwara et al., 2005; Ota et al., 2010), the KI catchment with low relief is characterized by lower stream gradients, greater drainage densities, and smaller zero-order catchment areas than NO. WS, one of the zero-order catchments included in KI, is less than 30 m long, whereas the length of NO catchment is 300 m. Referring to the results in the previous section, in KI, rainwater infiltrates deep into the weathered bedrock and does not contribute to storm runoff until about half of the ridge side from the middle of a hillslope in it, while in NO, the proportion of area not contributing to storm runoff would be much larger than in KI because of the longer distance to the ridge.

As described above, runoff response characteristics seem to be affected by long-term topographic development processes, even if the geology is almost the same. In the case of NO with high relief, it is assumed that faults associated with tectonic uplift created spatial divisions with discontinuous aquifers (Kosugi et al., 2011). In the case of KI, on the other hand, the bedrock structure may be relatively continuous, based on the small size of the zero-order catchment and the observation results by Katsura et al. (2014). However, the influence of the localized nature of the bedrock surface on runoff were already pointed out by a `fill and spill mechanism' in which shallow groundwater filled the concave topography of the bedrock surface, causing the downslope subsurface flow (Tromp-van Meerveld and McDonnell, 2006). Therefore, when a localized downslope flow occurs, the occurrence areas in the lower part of the catchment with shallow groundwater level are likely to be connected to each other and the downslope flow can develop. As a result, it is assumed that storm-runoff

contribution area in the lower part is divided from the infiltration area in the upper part. However, more detailed observational studies are needed to clarify the actual generation and development of the downslope flow.

Thus, it must be said that it is very difficult to estimate the location and mechanism of downslope flow system for granite KI, as was the case for sedimentary rock TY. When focusing on storm runoff response in a CWC, we can say that the role of the vertical system may be significant, as argued through our applications of the VZ model. However, the full picture of the runoff mechanism, which is divided into storm runoff and baseflow, must be regarded as another issue, in which the downslope system also plays a major role. In addition to detailed observational studies of runoff mechanisms, it will be necessary to explain the subsurface structure of the catchment in terms of long-term geomorphological and rock-weathering processes.

Finally, we would like to emphasize that the discussion on the runoff mechanism that leads to the catchment-specific diversity of runoff characteristics, including storm runoff and baseflow responses, has been only made possible by the proposal and applications of the VZ model. The runoff conversion process in a CWC is produced from the vertical system and calculated by the VZ model. The drainage rate from the bottom of the soil layer is distributed between storm runoff through the downslope flow and deep infiltration into the weathered bedrock. Hence, we can conclude that information obtained from the applications of the VZ model has provided a prerequisite for the discussion on diversity of runoff characteristics.

VI. Conclusion and perspectives

The runoff mechanism producing storm runoff responses in small mountainous catchments can be viewed as a structure that changes direction from vertical to downslope system, and in this paper, we proposed a runoff model based on the author's previous work assuming that vertical unsaturated flow plays an important role. In our VZ model, it is assumed the downslope system is not a major controller, and that the flow rate drained from the soil layer obtained by solving the Richards equation for the vertical system is simply integrated over the entire catchment using the distribution of soil layer thickness in it to produce storm runoff responses. The VZ model was used to calculate the runoff from three small mountainous catchments with information on soil layer thickness and soil physical properties, and the results were found to well simulate the observed storm runoff responses, including large rainfall events causing landslide occurrences.

In terms of runoff model applicability, there are countless models that calculate runoff under rainfall conditions, and the result of good applicability is not particularly significant. However, while there has been a strong tendency to assume that topographic effects such as slope length and gradient of downslope system dominate storm runoff responses (e.g., Beven and Kirkby, 1979; Shiiba et al., 2013), the VZ model has the significant feature of claiming that soil layer thickness and soil physical properties are dominant for large rainfall events. In this respect, this paper is believed to be significant in the history of runoff model development study.

Traditionally, how to resolve the discordance between observations and models has been an important goal of the hydrological research (e.g., McDonnell, 1990; Harman and Sivapalan, 2009). Therefore, in this paper, emphasis has been placed on discussing the results of the application of the VZ model in conjunction with observations on the runoff mechanism. The findings are itemized below.

1) The VZ model well simulated the runoff conversion processes of temporal variation between rainfall intensity and runoff rate on a small slope located in KI catchment and in CB1, a zero-order catchment of MR study site. These results showed the existence of a mechanism that produced rapid runoff responses from the vertical system into the stream through the sandy soil and bedrock fractures in the downslope system.

(2) The VZ model was applied to catchments of KT and MN in TY as well as SL, a valley-side slope in MN, and the calculated runoff rates were compared with those observed to examine the development of runoff contribution area. The results showed that during the period when the CWC (complete wet condition) areas were still isolated, the runoff rate was small due to the limited contribution area. However, when the CWC areas were interconnected by an additional rainfall event, the runoff rate increased, and as the cumulative rainfall increases, even areas with thicker soil layers became contribution areas, finally reaching a CAP (constant allocation period), which can explain the expansion of the storm runoff contribution area. However, the detailed mechanism of the downslope flow in the area of sedimentary rocks, which covered most of the TY catchment area, was still unclear, although fractures in the weathered bedrocks were assumed to be responsible for rapid groundwater drainage.

(3) In application to MR, the VZ model was also applied to the event in which a landslide occurred in CB1, and the storm runoff response was well simulated until just before the occurrence. Based on these results, it is hypothesized that "the reason why storm runoff response is mainly dominated by the vertical system is

that the capacity of the downslope flow system to drain groundwater is large enough to keep the soil layer stable for several hundred years or more.

(4) Unlike MR and TY in sedimentary rocks, the magnitude of runoff did not reach the same as that of rainfall in granite KI, even when the cumulative rainfall increases: the observed runoff rates were only about half of those calculated by the VZ model and well simulated by them. The mechanism for this phenomenon was estimated that "although the effect of storage fluctuation in the weathered bedrock was significant even under a CWC, the interception of infiltration into the bedrock by the shallow groundwater level within it in the lower part of the catchment caused the downslope flow producing storm runoff responses". Furthermore, the distribution ratio between storm runoff and baseflow was considered to be affected by the geomorphological evolutional process of a granite catchment.

Based on the above results, let us revisit the assumptions of the VZ model. It was assumed that there was no rise of the unconfined groundwater flow within the soil layer in a downslope system, and that an unsaturated zone remained in the layer even when cumulative rainfall was large, where vertical unsaturated flow was responsible for the storm runoff responses. This may seem an unrealistic assumption because hydrological observations often reported the rise of unconfined groundwater within the soil layer during rainfall (Kubota and Sivapalan, 1995; Tani et al., 2012) and the occurrence of overland flow (Gomi et al., 2008). However, the findings in this paper only demonstrate that the observed runoff conversion processes in CWCs are well explained by the Richards equation governing vertical unsaturated flow and never deny that groundwater table rise and overland flow occur as a reality in the field. Therefore, the author believes that applications of the VZ model with its bold assumptions have provided new information that will be useful in future discussions in hydrology. This is because the author is aware of the fact that difficult problems remain that cannot be explained by numerous runoff models proposed by simplifying runoff mechanisms with high complexity and heterogeneity in the downslope system. Although the VZ model is based on a vertical system, it is rather seen as a tool for estimating flow mechanisms of the downslope system. In this sense, the author believes that the current status of hillslope hydrology is still at the stage of "somehow exploring the mechanisms of downslope system based on the information obtained from observational results for the vertical system".

In order to explore the direction of future research on the runoff mechanisms of downslope system, let us review the information obtained in this paper on this system, taking TY, which was mainly composed of sedimentary rocks, as an example. The storm runoff responses under CWCs were well simulated when the maximum thickness of the soil layer in the VZ model was taken to be 2.5 m, and from this result, it was inferred that this layer was maintained as an unsaturated state and that soil moisture fluctuations there mainly controlled the runoff conversion process. However, the weathered bedrock layer was found to extend deeper, and rapid and large groundwater level fluctuations corresponding to storm runoff responses were observed in CWCs (Hosoda and Tani, 2016). In the highly heterogeneous weathered bedrock containing fractures, interactions between the capillary-force dominated unsaturated state and the hydraulic-pressure dominated saturated state might produce temporal fluctuations of groundwater level. Furthermore, because fractures have different hydraulic functions as open-channel flow and closed-conduit flow (Tsutsumi et al., 2005a; b), the function of the fracture network may change with time as the water table fluctuates. The flow in the downslope system is thought to be caused by the runoff mechanism in such a heterogeneous subsurface structure.

Then, why is the subsurface structure leading to the flow of the downslope system heterogeneous? This question may only be answered by the evolutional processes of the mountain topography and subsurface structure including soil layers at a long timescale, as mentioned in our discussions on the occurrence or non-occurrence of landslide in MR and the comparison of KI and NO runoff mechanisms in granite catchments (Matsushi et al., 2016; Watakabe et al., 2019). In order to find a direction for future research on this issue, the author, with the support of the Japan Society of Hydrology and Water Resources, established a study group on "Researching consistencies between runoff processes and geomorphological evolutional processes in mountainous regions" from 2021 to 2023, and conducted online workshops with the participation of researchers from various fields including hydrology, geomorphology, and erosion control. Refer two reports in Journal of Japan Society of Hydrology and Water Resources (Tani et al., 2022; 2024) and one report in Transactions, Japanese Geomorphological Union (Iida et al., 2023). The author hopes that this paper will serve as a basis for future discussions on this interdisciplinary subject.

Acknowledgements

This paper is based on discussions in the study group "Researching consistencies between runoff processes and geomorphological evolutional processes in mountainous regions" of the Japan Society of Hydrology and Water Resources. I would like to thank

Dr. Tomoyuki Iida (former National Research Institute for Earth Science and Disaster Resilience), Dr. Taro Uchida (University of Tsukuba), Dr. Kenta Iwasaki (Forestry and Forest Products Research Institute), and about 150 participants in the online workshop for their useful comments. We thank Dr. William E. Dietrich (University of California, Berkeley) for his detailed comments on the discussion of the Mettman Ridge study site CB1, Dr. Suzanne P. Anderson (University of Colorado) for providing hydrological data with comments on the MREX hydrologic observations, and Dr. Masanori Katsuyama (Kyoto Prefectural University) for providing soil layer distribution data of the Kiryu Experimental Watershed. We would also like to express our sincere gratitude to the anonymous reviewers for their careful reviewing of the manuscript, which greatly improved the content of the manuscript by providing a vast number of valuable suggestions. The research was supported by the above research group expenses and by Grant-in-Aid for Scientific Research (19K04632) " Development of a storm-runoff model based on the measurements of saturated-unsaturated flow on a hillslope (led by Nagahiro Kojima)".

References

Anderson AE, Weiler M, Alila Y, Hudson RO. 2009. Subsurface flow velocities in a hillslope with lateral preferential flow. Water Resources Research 45: W11407. DOI: 10.1029/2008WR007121.

Anderson SP, Dietrich WE, Montgomery DR, Torres R, Conrad ME, Loague K. 1997. Subsurface flow paths in a steep, unchanneled catchment. Water Resources Research 33: 2637-2653. DOI: 10.1029/97WR02595.

Asano Y, Uchida T, Tomomura M. 2020. A novel method of quantifying catchmendanjot-wide average peak propagation speed in hillslopes: Fast hillslope responses are detected during annual floods in a steep humid catchment. Water Resources Research 56, e2019WR025070. DOI: 10.1029/2019WR025070.

Beven K, Germann P. 2013. Macropores and water flow in soils revisited. Water Resources Research 49: 3071-3092. DOI: 10.1002/wrcr.20156.

Beven K, Kirkby M. 1979. A physically based, variable contributing area model of basin hydrology. Hydrological Sciences Bulletin 24: 43-69. DOI: 10.1080/02626667909491834.

Danjo T. 2017. Mechanisms of landslide hazards by heavy storms and their prediction methods. Journal of Japan Society for Safety Engineering 56:464-469 (In Japanese. Title is translated by the present author). DOI: : 10.18943/safety.56.6_463.

Dusek J, Vogel T, Dohnal M, Gerke HH. 2012. Combining dual-continuum approach with diffusion wave model to include a preferential flow component in hillslope scale modeling of shallow subsurface runoff. Advances in Water Resources 44: 113–125. DOI: 10.1016/j.advwatres.2012.05.006.

Ebel BA, Loague K, Vanderkwaak JE, Dietrich WE, Montgomery DR, Torres R, Anderson SP. 2007. Near-surface hydrologic response for a steep unchannelled catchment near Coos Bay, Oregon: 2. Physics-based simulations. American Journal of Science 307: 709-748. DOI: 10.2475/04.2007.03.

Freeze RA. 1972. Role of subsurface flow in generating surface runoff 2. Upstream source areas. Water Resources Research 8: 1272-1283. DOI: 10.1029/WR008i005p01272.

Fujimura K, Iseri Y, Okada S Kanae S, Murakami M. 2016. Analytical study toward reducing uncertainty of parameters in the storage-discharge function. Proceedings of Japan Society of Civil Engineers, (G) Environmental systems research 72(5): I_35-I_43 (In Japanese with English abstract). DOI: 10.2208/jscejer.72.I_35.

Fujita M. 1981. The impact of variations of slope length on storage-discharge relationships. Proceedings of the Japan Society of Civil Engineers 314: 75-86 (In Japanese). DOI: 10.2208/jscej1969.1981.314_75.

Fujiwara O, Yanagida M, Sanga T, Moriya T. 2005. Researches on tectonic uplift and denudation with relation to geological disposal of HLW in Japan. Journal of nuclear fuel cycle and environment11(2): 113-124. DOI: 10.3327/jnuce.11.113.

Fukushima Y. 1988. A model of river flow forecasting for a small mountain catchment. Hydrological Processes 2: 167-185. DOI: 10.1002/hyp.3360020207.

Fukushima Y. 2006. The role of gorest on the hydrology of headwater wetlands. In: Environmental Role of Wetlands in Headwaters, Krecek J, Haigh M (eds). Springer, Dordrecht; 17-47.

Fukushima Y, Suzuki M. 1985. Hydrological cycle model for mountain watershed and its application to the continuous 10 years records at intervals of bot a day and an hour of Jiryu Watershed, Shiga Prefecture. Bulletin of the Kyoto University Forests 57: 162-185. https://agriknowledge.affrc.go.jp/RN/2030323022.pdf.

Fukushima, Y. 1987. Effects of stream flow on reforestation in granitic hilly mountain. Suirikagaku 31(4): 17–34 (In Japanese). DOI: 10.20820/suirikagaku.31.4_17.

Gomi T, Asano Y, Uchida T, Onda Y, Sidle RC, Miyata S, Kosugi K, Mizugaki S, Fukuyama T, Fukushima T. 2010. Evaluation of storm runoff pathways in steep nested catchments draining a Japanese cypress forest in central Japan: a geochemical approach. Hydrological Processes 24: 550-566. DOI: 10.1002/hyp.7550.

Gomi T, Sidle RC, Ueno M, Miyata S, Kosugi K. 2008.

Characteristics of overland flow generation on steep forested hillslopes of central Japan. Journal of Hydrology 361:275-290.
DOI: 10.1016/j.jhydrol.2008.07.045.

Harman C, Sivapalan M. 2009. A similarity framework to assess controls on shallow subsurface flow dynamics in hillslopes, Water Resources Research 45: W01417. DOI: 10.1029/2008WR007067.

Hewlett JD, Hibbert AR. 1967. Factors affecting the response of small watersheds to precipitation in humid areas. In Proceedings of the International Symposium on Forest Hydrology, Sopper WE, Lull HW (eds), Pennsylvania State University: Pergamon; 275-290.

Hopmans JW, van Genuchten MT. 2005. Vadose zone: Hydrological process. In Encyclopedia of Soils in the Environment, Hillel D (ed). Elsevier: Oxford; 209-216.

Horton JH, Hawkins RH. 1965. Flow path of rain from the soil surface to the water table. Soil Science 100: 377-383.

Hosoda I, Tani M. 2016. Influence of moisture fluctuations in thick, weathered bedrock layers on rainfall-runoff response in a small, forested catchment underlain by Paleozoic sedimentary rocks in Japan. Transactions, Japanese Geomorphological Union 37:465-492 (In Japanese with English abstract).

Iida T, Tani M,Uchida T, Iwasaki K. 2023. Introduction of interdisciplinary study group on hydro-geomorphology : Report of the 3rd and 4th meeting of study group on consistency between mountain runoff processes and landform development processes. Transactions, Japanese Geomorphological Union 44(1): 33-41 (In Japanese).

Iida T. 2012. Slope failure knowledge needed by engineers. Kajima Institute Publishing; 233 (In Japanese. Title is translated by the present author).

Iwasaki K, Katsuyama M, Tani M. 2015. Contributions of bedrock groundwater to the upscaling of storm-runoff generation processes in weathered granitic headwater catchments. Hydrological Processes 29: 1535-1548. DOI: 10.1002/hyp.10279.

Iwasaki K, Katsuyama M, Tani M. 2020. Factors affecting dominant peak-flow runoff-generation mechanisms among five neighbouring granitic headwater catchments. Hydrological Processes 34: 1154-1166. DOI: 10.1002/hyp.13656.

Japanese Geotechnical Society. 2004. Geotechnical Survey Methods and Explanations. Japanese Geotechnical Society; 889 (In Japanese. Title is translated by the present author).

Kadoya M. 1979. Runoff analysis techniques Part 1 – Storm runoff phenomena and their measurement and analysis. Journal of the Agricultural Engineering Society, Japan 47: 811-821 (In Japanese. Title is translated by the present author).
DOI: 10.11408/jjsidre1965.47.10_811.

Kaki T. 1958. On the sand running-down and sabo planning. Shin-Sabo 31: 19-22 (In Japanese).
DOI: 10.11475/sabo1948.1958.31_19.

Kashiwaya K, Yoneda T. 2004. Crack pattern changes observed in rock weathering and its characterization by multifractal analysis. Journal of the Japan Society of Engineering Geology. 45：90-100 (In Japanese with English abstract).
DOI: 10.5110/jjseg.45.90.

Katsura S, Kosugi K, Yamakawa Y, Mizuyama T. 2014. Field evidence of groundwater ridging in a slope of a granite watershed without the capillary fringe effect. Journal of Hydrology 511: 703-718.
DOI: 10.1016/j.jhydrol.2014.02.021.

Katsura S, Kosugi K, Yamamoto N, Mizuyama T. 2006. Saturated and unsaturated hydraulic conductivities and water retention characteristics of weathered granitic bedrock. Vadose Zone Journal 5: 35–47. DOI: 10.2136/vzj2005.0040.

Katsuyama M, Ohte N, Kabeya N. 2005. Effects of bedrock permeability on hillslope and riparian groundwater dynamics in a weathered granite catchment. Water Resources Research 41. W01010. DOI:10.1029/2004WR003275.

Katsuyama M, Ohte N, Kosugi Y, Tani M. 2021. The Kiryu Experimental Watershed: 50-years of rainfall-runoff data for a forest catchment in central Japan. Hydrological Processes 35: e14104.
DOI: 10.1002/hyp.14104.

Katsuyama M, Tani, M Nishimoto S. 2010. Connection between streamwater mean residence time and bedrock groundwater recharge/discharge dynamics in weathered granite catchments. Hydrological Processes 24: 2287-2299. DOI: 10.1002/hyp.7741.

Kikui T, Senoo K. 2004. Warning and evacuation standards informative to the public for the prevention of sediment-related disasters. Internationales Symposion INTERPRAEVENT RIVA/TRIENT, IX/89-IX/99. http://www.interpraevent.at/palm-cms/upload_files/Publikationen/Tagungsbeitraege/2004_4_IX-89.pdf.

Kimura T. 1961. The flood runoff analysis method by the storage function model. The Public Works Research Institute, Ministry of Construction (In Japanese).

Kimura T. 1978. The recent progresses in storage function method. Proceedings of the Japanese Conference on Hydraulics 22: 191-196.
DOI: 10.2208/prohe1975.22.191.

Kitahara H. 1992. Characteristics of pipe flow in the forest soil. Journal of Japan Society of Hydrology and Water Resources 5: 15-25 (In Japanese. Title is translated by the present author).
DOI: 10.3178/jjshwr.5.1_15.

Kitahara H. 1993. Characteristics of pipe flow in

forested slopes, Exchange Processes at the Land Surface for a Range of Space and Time Scales, IAHS Publ. 212: 235-242.
Kosugi K. 1996. Lognormal distribution model for unsaturated soil hydraulic properties. Water Resources Research 32: 2697-2703. DOI: 10.1029/96WR01776.
Kosugi K. 1999. New index to evaluate water holding capacity of forest soils. Journal of the Japanese Forestry Society 81: 226-235 (In Japanese with English abstract). DOI: 10.11519/jjfs1953.81.3_226.
Kosugi K, Fujimoto M, Katsura S, Kato H, Sando Y, Mizuyama T. 2011. Localized bedrock aquifer distribution explains discharge from a headwater catchment. Water Resources Research 47. W07530. DOI: 10.1029/2010WR009884.
Kosugi K, Katsura S, Katsuyama M, Mizuyama T. 2006. Water flow processes in weathered granitic bedrock and their effects on runoff generation in a small headwater catchment. Water Resources Research 42. W02414. DOI: 10.1029/2005WR004275.
Kosugi Y, Takanashi S, Ueyama M, Ohkubo S, Tanaka H, Matsumoto K, Yoshifuji N, Ataka M, Sakabe A. 2013. Determination of the gas exchange phenology in an evergreen coniferous forest from 7 years of eddy covariance flux data using an extended big-leaf analysis. Ecological Research 28: 373–385. DOI: 10.1007/s11284-012-1019-4.
Kubota J, Sivapalan M. 1995. Towards a catchment-scale model of subsurface runoff generation based on synthesis of small-scale process-based modelling and field studies. Hydrological Processes 9: 541-554. DOI: 10.1002/hyp.3360090506.
Laurance WF. 2007. Forests and floods. Nature 449:409-410. https://www.nature.com/articles/449409a.
Lehman P, Hinz C, McGrath G, Tromp-van Meerveld HJ, McDonnell JJ. 2007. Rainfall threshold for hillslope outflow: an emergent property of flow pathway connectivity. Hydrology and Earth System Sciences 11: 1047-1063. DOI: 10.5194/hess-11-1047-2007.
Liang W, Kosugi K, Mizuyama T. 2009. A three-dimensional model of the effect of stemflow on soil water dynamics around a tree on a hillslope. Journal of Hydrology 366: 62–75. DOI: 10.1016/j.jhydrol.2008.12.009.
Liu YJ, Chiu YY, Tsai F, Chen SC. 2022. Analysis of landslide occurrence time via rainfall intensity and soil water index ternary diagram. Landslides 19: 2823-2837. DOI: 10.1007/s10346-022-01944-1.
Matsushi Y, Toyama M, Matsuzaki H, Chigira M. 2016. Simulation of soil production and transport for prediction of location and magnitude of shallow landslides. Transactions, Japanese Geomorphological Union 37：427-453 (In Japanese with English abstract).
McDonnell JJ. 1990. A Rationale for old water discharge through macropores in a steep, humid catchment. Water Resources Research 26: 2821-2832. DOI: 10.1029/WR026i011p02821.
McDonnell JJ. 2009. Hewlett, J.D. and Hibbert, A.R. 1967: Factors affecting the response of small watersheds to precipitation in humid areas. In Sopper, W.E. and Lull, H.W., editors, Forest hydrology. Progress in Physical Geography 33: 288-293. DOI: 10.1177/0309133309338118.
McDonnell JJ, Beven K. 2014. Debates—The future of hydrological sciences: A (common) path forward? A call to action aimed at understanding velocities, celerities and residence time distributions of the headwater hydrograph. Water Resources Research 50: 5342–5350. DOI:10.1002/2013WR015141.
Montgomery DR, Dietrich WE, Torres R, Anderson SP, Heffner JT, Loague K. 1997. Hydrologic response of a steep, unchanneled valley to natural and applied rainfall. Water Resources Research 33: 91-109. DOI: 10.1029/96WR02985.
Montgomery DR, Schmidt KM, Dietrich WE, McKean J. 2009. Instrumental record of debris flow initiation during natural rainfall: Implications for modeling slope stability. Journal of Geophysical Research 114. DOI:10.1029/2008JF001078.
Mosley MP 1982. Subsurface flow velocities through selected forest soils, South Island, New Zealand. Journal of Hydrology 55: 65-92. DOI: 10.1016/0022-1694(82)90121-4.
Musiake K. 1982. Characteristics of water resources in headwater catchments of Tone River. Urban Kubota 19: 46-51 (In Japanese. Title is translated by the present author). https://www.kubota.co.jp/urban/data/19.pdf
Musiake K, Takahasi Y, Ando Y. 1981. Effects of basin geology on river-flow regime in mountainous areas of Japan. Proceedings of the Japan Society of Civil Engineers 309：51-62 (In Japanese). DOI: 10.2208/jscej1969.1981.309_51.
Noguchi S, Abd Rahim N, Zulkifli Y, Tani M, Sammori T. 1997. Rainfall-runoff responses and roles of soil moisture variations to the response in tropical rain forest, Bukit Tarek, Peninsular Malaysia. Journal of Forest Research 2: 125-132. DOI: 10.1007/BF02348209.
Ohta T, Fukushima Y, Suzuki M. 1983. Research on runoff from hillsides by one-dimensional transient saturated-unsaturated flow. Journal of the Japanese Forestry Society 65: 125-134 (In Japanese with English abstract). DOI: 10.11519/jjfs1953.65.4_125.
Ohta R, Matsushi Y, Matsuzaki H. 2022. Use of terrestrial cosmogenic 10Be to quantify

anthropogenic sediment yield from mountainous watersheds: Application in reconstructing environmental change in the Tanakami Mountains, central Japan. Geomorphology 405: 108201. DOI: 10.1016/j.geomorph.2022.108201.

Ohte N, Tokuchi N, Suzuki M. 1995. Biogeochemical influences on the determination of water chemistry in a temperate forest basin: Factors determining the pH value. Water Resources Research 31, 2823-2834. DOI: 10.1029/95WR02041.

Okada K. 2002. Soil water index. Weather service bulletin 69(5): 67-100 (In Japanese. Title is translated by the present author).

Okada K. 2016. Outbreak timing of the sediment disasters judging from soil water index. Technical note of the National Research Institute for Earth Science and Disaster Prevention 405: 51-60 (In Japanese with English abstract).

Onda Y, Komatsu Y, Tsujimura M, Fujihara J. 2001. The role of subsurface runoff through bedrock on storm flow generation. Hydrological Processes 15: 1693-1706. DOI: 10.1002/hyp.234.

Ota Y, Koike K, Chinzei K, Nogami M, Machida H, MatsudabT. 2010. Geomorphology of the Japanese Archipelago. University of Tokyo Press; 204 (In Japanese. Title is translated by the present author).

Padiyedath SG, Kawamura A, Amaguchi H, Azhikodan G. 2018. Effect of lag time in Kimura's storage function model on hydrograph reproducibility for an urban watershed compared with Prasad's model. Journal of the Japan Society of Civil Engineers, (G) Environmental systems research 74(5): I69-I77. DOI: 10.2208/jscejer.74.I_69

Sakabe A, Takahashi K, Azuma W, Itoh M, Tateishi M, Kosugi Y. 2021. Controlling factors of seasonal variation of stem methane emissions from Alnus japonica in a riparian wetland of a temperate forest. Journal of Geophysical Research: Biogeosciences 126: e2021JG006326. DOI: 10.1029/2021JG006326.

Schmidt KM. 1999. Root strength, colluvial soil depth, and colluvial transport on landslide-prone hillslopes. University of Washington. ProQuest Dissertations Publishing, 9944177; 298. https://www.proquest.com/docview/304540934?pq-origsite=gscholar&fromopenview=true.

Science Council of Japan. 2001. Evaluation of the multifunctional role of agriculture and forests in relation to the global environment and human life (Report) (In Japanese. Title is translated by the present author). https://www.scj.go.jp/ja/info/kohyo/pdf/shimon-18-1.pdf.

Science Council of Japan, 2011. Academic assessment of river runoff model and unregulated peak discharge validation (Response) (In Japanese. Title is translated by the present author.) https://www.scj.go.jp/ja/info/kohyo/pdf/kohyo-21-k133-1-2.pdf.

Senoo K, Godai H, Hara Y, Shiojima Y. 1985. Rainfall indexes for debris flow warning evacuating program. Journal of the Japan Society of Erosion Control Engineering 38(2): 16-21 (In Japanese). DOI: 10.11475/sabo1973.38.2_16.

Shiiba M, Tachikawa Y, Ichikawa Y. 2013. Hydrology and Water Engineering. Kyoto University Press; 615 (In Japanese. Title is translated by the present author).

Shimizu T. 1980. Rc1ation between scanty runoff from mountainous watershed and geology, slope and vegetation. Bulletin of Forestry and Forest Products Institute 310: 109-128 (In Japanese with English abstract). https://www.ffpri.affrc.go.jp/labs/kanko/310-5.pdf

Sidle RC., Kitahara H, Terajima T, Nakai Y. 1995. Experimental studies on the effects of pipeflow on throughflow partitioning. Journal of Hydrology 165: 207-219. 10.1016/0022-1694(94)02563-Q.

Šimůnek J, Šejna M, Saito H, Sakai S, van Genuchten MT. 2013. The Hydrus-1D software package for simulating the movement of water, heat, and multiple solutes in variably saturated media, Version 4.17, HYDRUS Software Series 3. Department of Environmental Sciences, University of California Riverside: Riverside; 344.

Sivapalan M. 2003. Process complexity at hillslope scale, process simplicity at the watershed scale: is there a connection? Hydrological Processes 17: 1037-1041. DOI: 10.1002/hyp.5109.

Sklash MG, Farvolden RN. 1979. The role of groundwater in storm runoff, Journal of Hydrology 43: 45-65. DOI: 10.1016/0022-1694(79)90164-1.

Sugawara M. 1985. Tank model – For the derivation of river discharge from rainfall -. Journal of Geography (Chigaku Zasshi) 94: 209-221 (In Japanese with English abstract). DOI: 10.5026/jgeography.94.4_209

Sugiyama H, Kadoya M. 1988. Discussion on Parameters of the Storage Function Model. Journal of the Agricultural Engineering Society, Japan 133:11-18 (In Japanese with English abstract). DOI: 10.11408/jsidre1965.1988.11.

Sugiyama H, Kadoya M, Nagai A, Lansey K. 1997. Evaluation of the storage function model parameter characteristics. Journal of Hydrology 191: 332-348. DOI: 10.1016/S0022-1694(96)03026-0.

Supraba I, Yamada T. 2015. Potential water storage capacity of mountainous catchments based on catchment characteristics. Journal of the Japan Society of Civil Engineer, Ser. B1 (Hydraulic Engineering) 71 (4) ：I_151-I_156. DOI: 10.2208/jscejhe.71.I_151.

Suzuki M. 1980. Evapotranspiration from a small catchment in hilly mountains (I) Seasonal variations in evapotranspiration, rainfall interception and

transpiration. Journal of the Japanese Forestry Society 62: 46-53. DOI: 10.11519/jjfs1953.62.2_46.

Suzuki M. 1984. The properties of a base-flow recession on small mountainous watersheds (II) Influence of evapotranspiration on recession hydrographs. Journal of the Japanese Forestry Society 66: 211-218 (In Japanese with English abstract). DOI: 10.11519/jjfs1953.66.6_211.

Suzuki M, Fukushima Y, Takei A, Kobashi S. 1979. The critical rainfall for the disasters caused by debris movement. Journal of the Japan Society of Erosion Control Engineering 31(3): 1-7 (In Japanese with English abstract). DOI: 10.11475/sabo1973.31.3_1.

Takagi F, Matsubayashi U. 1979. On the non-linearity of sub-surface and groundwater-runoff. Proceedings of the Japan Society of Civil Engineers 283: 45-55 (In Japanese). DOI: 10.2208/jscej1969.1979.283_45.

Takahashi S. 2019. Flood control and water utilization functions of forest and the limitations. Dam and green dam (Musiake K, Ohta T, eds), Nikkei Business Publications; 45-68 (In Japanese. Title is translated by the present author).

Takasao T, Shiiba M. 1988. Incorporation of the effect of concentration of flow into the kinematic wave equations and its applications to runoff system lumping. Journal of Hydrology 102:301-322. DOI: 10.1016/0022-1694(88)90104-7.

Tamai K. 2014. Comparison of flow regimes from watersheds with different forest ages. Suirikagaku 57(6): 73-91 (In Japanese. Title is translated by the present author). DOI: 10.20820/suirikagaku.57.6_73.

Tamai K, Boyer EW, Iida S, Carlyle-Moses DE, Levia DF. 2020. Forest influences on streamflow: Case studies from the Tatsunokuchi-Yama Experimental Watershed, Japan, and the Leading Ridge Experimental Watershed, USA. In Forest-Water Interactions. Leivia DF (ed), Springer, Cham, Switzerland; 519-536.

Tani M. 1982. The properties of a water-table rise produced by a one-dimensional, vertical, unsaturated flow. Journal of the Japanese Forest Society 64: 409-418 (In Japanese with English abstract). DOI: 10.11519/jjfs1953.64.11_409.

Tani M. 1985a. Analysis of one-dimensional, vertical, unsaturated flow in consideration of runoff properties of a mountainous watershed. Journal of the Japanese Forest Society 67: 449-460, 1985 (In Japanese with English abstract). DOI: 10.11519/jjfs1953.67.11.

Tani M. 1985b. The effects of soil physical properties on the groundwater-table rise. Proceedings of the International Symposium. On Erosion, Debris Flow, and Disaster Prevention, Takei A (ed)., The Erosion Control Engineering Society, Japan, Tokyo, 361–365.

Tani M. 1996. An approach to annual water balance for small mountainous catchments with wide spatial distributions of rainfall and snow water equivalent. Journal of Hydrology 183: 205-225. DOI: 10.1016/0022-1694(95)02983-4.

Tani M. 1997. Runoff generation processes estimated from hydrological observations on a steep forested hillslope with a thin soil layer. Journal of. Hydrology 200: 84-109. DOI: 10.1016/S0022-1694(97)00018-8.

Tani M. 2008. Analysis of runoff storage relationships to evaluate the runoff-buffering potential of a sloping permeable domain. Journal of Hydrology 360: 132-146. DOI: 10.1016/j.jhydrol.2008.07.023.

Tani M. 2016. Science of Water, Soil, and Forest. Kyoto University Press; 243 (In Japanese. Title is translated by the present author).

Tani M. 2013. A paradigm shift in stormflow predictions for active tectonic regions with large-magnitude storms: generalisation of catchment observations by hydraulic sensitivity analysis and insight into soil-layer evolution. Hydrology and Earth System Sciences 17: 4453-4470. DOI: org/10.5194/hess-17-4453-2013.

Tani M. 2018. Influences of forest on the water cycle. In Forest and Hazards, Nakamura F, Kikuzawa K (eds). Kyoritsu Shuppan; 24-77 (In Japanese. Title is translated by the present author).

Tani M, Abe T, Hattori S. 1988. Analysis of sediment transport in a torrent in a weathered granite mountain. Journal of the Japan Society of Erosion Control Engineering 41(2): 13-20 (In Japanese). DOI: 10.11475/sabo1973.41.2_13.

Tani M, Fujimoto, M, Katsuyama M, Kojima N, Hosoda I, Kosugi K, Kosugi Y, Nakamura S. 2012. Predicting the dependencies of rainfall-runoff responses on human forest disturbances with soil loss based on the runoff mechanisms in granitic and sedimentary-rock mountains. Hydrological Processes 26: 809–826. DOI: 10.1002/hyp.8295.

Tani M, Hosoda I. 2012. Dependence of annual evapotranspiration on a long natural growth of forest and vegetation changes. Journal of Japan Society of Hydrology and Water Resources 25: 71-88 (In Japanese with English abstract). DOI: 10.3178/jjshwr.25.71.

Tani M, Iida T, Uchida T, Iwasaki K. 2022. Report of the 1st and 2nd online meetings in workshop on researching consistencies between runoff processes and geomorphological evolutional processes in mountainous regions. Journal of Japan Society of Hydrology and Water Resources 35: 349-357 (In Japanese). https://www.jstage.jst.go.jp/article/jjshwr/35/5/35_35.349/_pdf/-char/ja.

Tani M, Iida T, Uchida T, Iwasaki K. 2024. Final report of 'the workshop on researching consistencies between runoff processes and geomorphological evolutional processes in mountainous regions In Japanese) Japan Society of Hydrology and Water Resources 37 (in press).

Tani M, Matsushi Y, Sayama T, Sidle RC, Kojima N. 2020. Characterization of vertical unsaturated flow reveals why storm runoff responses can be simulated by simple runoff-storage relationship models. Journal of Hydrology 588: 124982. DOI: 10.1016/j.jhydrol.2020.124982.

Torres R, Dietrich WE, Montgomery DR, Anderson SP, Loague K. 1998. Unsaturated zone processes and the hydrologic response of a steep, unchanneled catchment. Water Resources Research 34: 1865-1879. DOI: 10.1029/98WR01140.

Tromp-van Meerveld HJ, McDonnell JJ. 2006. Threshold relations in subsurface stormflow: 2. The fill and spill hypothesis. Water Resources Research 42. DOI:10.1029/2004WR003800.

Tsukamoto Y, Matsuoka M, Kurihara K. 1978. Study on the growth of stream channel (VI) Landslides as the process of erosional development of basin morphology. Journal of the Japan Society of Erosion Control Engineering 30(4): 25-32 (In Japanese). DOI: 10.11475/sabo1973.30.4_25.

Tsukamoto Y, Ohta T. Runoff process on a steep forested slope. Journal of Hydrology 102: 165-178, 1988. DOI: org/10.1016/0022-1694(88)90096-0.

Tsutsumi D, Fujita M, Sidle RC. 2005a. Preferential flow through cracks in weathered bedrock and slope stability : numerical modeling. Annual Journal of Hydraulic Engineering, JSCE 49: 1039-

Tsutsumi D, Sidle RC, Kosugi K. 2005b. Development of a simple lateral preferential flow model with steady state application in hillslope soils. Water Resources Research 41 (12). DOI: 10.1029/2004WR003877.

Uchida T, Asano Y, Ohte N, Mizuyama T. 2003. Analysis of flowpath dynamics in a steep unchannelled hollow in the Tanakami Mountains of Japan. Hydrological Processes 17: 417-430. DOI: 10.1002/hyp.1133.

Uemura S, Hiramatsu S, Suzuki H. 2022. Future changes in slope failure caused by climate change. Landslides 59: 237-247. https://www.jstage.jst.go.jp/article/jls/59/6/59_237/_pdf.

Watakabe T, Matsushi Y. 2019. Lithological controls on hydrological processes that trigger shallow landslides: Observations from granite and hornfels hillslopes in Hiroshima, Japan. Catena 180: 55-68. DOI: 10.1016/j.catena.2019.04.010.